Laboratory investigation of the Bruun Rule and beach response to sea level rise

Alexander L. Atkinson[1*], Tom. E. Baldock[1], Florent Birrien[1], David P. Callaghan[1], Peter Nielsen[1], Tomas Beuzen[2], Ian L. Turner[2], Chris E. Blenkinsopp[3], Roshanka Ranasinghe[1,4,5,6].

[1] School of Civil Engineering, University of Queensland, St Lucia, QLD, 4072, Australia.

[2] Water Research Laboratory, School of Civil and Environmental Engineering, UNSW Sydney, NSW 2052, Australia.

[3] Water, Environment and Infrastructure Resilience Research Unit, Department of Architecture and Civil Engineering, University of Bath, Bath BA2 7AY, UK.

[4] Department of Water Science and Engineering, UNESCO-IHE, PO Box 3015, 2610 DA Delft, The Netherlands. R.Ranasinghe@unesco-ihe.org (Ph: +31 646 843 096)

[5] Water Engineering and Management, Faculty of Engineering Technology, University of Twente, PO Box 217, 7500 AE Enschede, The Netherlands

[6] Harbour, Coastal and Offshore Engineering, Deltares, PO Box 177, 2600 MH Delft, The Netherlands.

Abstract

Rising sea levels are expected to cause widespread coastal recession over the course of the next century. In this work, new insight into the response of sandy beaches to sea level rise is obtained through a series of comprehensive experiments using monochromatic and random waves in medium scale laboratory wave flumes.~~Beach response to sea level rise is investigated experimentally with monochromatic and random waves in medium scale laboratory wave flumes.~~ Beach profile development from initially planar profiles, and a 2/3 power law profile, exposed to wave conditions that formed barred or bermed profiles and subsequent profile development following rises in water level and the same wave conditions are presented. Experiments assess profile response to a step-change in water level as well as the influence of sediment deposition above the still water level (e.g. overwash). A continuity based profile translation model (PTM) is applied to both idealised and measured shoreface profiles, and is used to predict overwash and deposition volumes above the shoreline. Quantitative agreement with the Bruun Rule (and variants of it) is found for measured shoreline recession for both barred and bermed beach profiles. There is some variability between the profiles at equilibrium at the two different water levels. Under these idealised conditions, deviations between the original Bruun Rule, the modification

by Rosati et al. (2013) and the PTM model predictions are of the order of 15% and all these model predictions are within ±30% of the observed shoreline recession. Measurements of the recession of individual contour responses, such as the shoreline, may be subject to local profile variability; therefore, a measure of the mean recession of the profile is also obtained by averaging the recession of discrete contours throughout the active profile. The mean recession only requires conservation of volume, not conservation of profile shape, to be consistent with the Bruun Rule concept, and is found to be in better agreement with all three model predictions than the recession measured at the shoreline.

Keywords: Bruun Rule; sea level rise; coastal erosion; equilibrium profiles; sediment transport; beach morphodynamics

1. Introduction

With the recent increased rates of sea level rise (Hay et al., 2015), potential future shoreface response to changing water levels are a persistent concern worldwide. There remains a lack of suitably long-term measurements of shoreface profile change over timescales associated with sea-level-rise, henceforth *SLR* (Leatherman et al., 2000). As an alternative to obtaining natural or prototype data, smaller-scale physical models often behave in qualitatively similar ways to prototype beaches and shorefaces, forming the same characteristic features at a wide range of scales (Hughes, 1993; van Rijn et al., 2011). Reduced scale modelling can provide valuable information on factors that influence shoreface responses to *SLR*, such as overwash or onshore transport in deeper water, with the benefits of a controllable environment and accelerated timescales. Both overwash and onshore transport in deeper water have recently been proposed as additional mechanisms to be considered alongside the classical Bruun Rule (Bruun, 1962; Rosati et al., 2013; Dean and Houston, 2016).

The term 'Bruun Rule' was first coined by Schwartz (1967) as a result of experiments testing Bruun's (1962) model. It is perhaps the most well-known and common approach used to predict shoreline recession under *SLR*. The basis for the Bruun Rule is related to earlier work on natural beach profiles (Bruun, 1954), which were shown to exhibit a monotonic concave-up mean profile about which natural beach profiles fluctuate over time. The mean (also commonly referred to as a dynamic equilibrium) subaqueous profile shape (Figure 1) has the form:

$$h = A(x_{sl} - x)^{2/3} \tag{1}$$

for $x \leq x_{sl}$, where h is the water depth, with an origin seaward of the offshore limit of wave influence (h_*), x is the cross-shore location, x_{sl} is the still water shoreline location and A [$m^{1/3}$] is a scaling parameter influenced by controls such as sedimentology and wave climate (e.g. Bruun, 1954; Dean, 1991; Short, 1999). The offshore limit is the location where wave driven sediment transport ceases and the corresponding depth h_* is a time dependent variable that is expected to increase with time due to the increased likelihood of larger waves (Hallermeier, 1981); the concept implies that sediment at depths

64 greater than h_* is essentially unavailable through wave driven processes and this defines the seaward
65 location of the active profile. Bruun (1962) used this concept and reasoned that if a mean shoreface
66 profile in dynamic equilibrium with a quasi-steady wave climate is to be maintained relative to the still
67 water level in the presence of *SLR*, sediment can only come from landward of the offshore limit. This
68 results in a net-seaward sediment transport and a landward shift of the active profile to facilitate raising
69 the entire active profile by *SLR*, leading to the following formula which has become known as the Bruun
70 Rule:

$$R = SLR\frac{W}{B + h_*} \tag{2}$$

71 where all components have units of length. *R* is the recession of the profile (negative values indicating
72 progradation), *W* is the horizontal length of the cross-shore active profile, with an onshore limit typically
73 corresponding to a berm with a vertical face at the shoreline and horizontal crest, for which, *B* is the
74 berm height above the zero-datum, mean sea level (in the field) or still water level (in the lab). All
75 parameters are depicted in Figure 1. Figure 1 also demonstrates the coordinate reference system used in
76 the present work. The cross-shore horizontal origin, $x = 0$ m, is located seaward of the offshore limit of
77 profile change, and in the laboratory, it is fixed over the exposed flume bed in the laboratory
78 experiments. The vertical origin, $z = 0$ m, is located at the initial water level; therefore, when the water
79 level rises, the still water level is at the elevation z = SLR.

80 The Bruun Rule was developed under the assumption of a dynamic equilibrium profile, which is
81 the long-term mean profile, shaped under a quasi-steady wave climate. To determine the existence and
82 shape of the dynamic equilibrium profile requires a dataset of regularly measured profiles that captures
83 the envelope of profile change that occurs with all water level and climate fluctuations (e.g. storms,
84 spring-neap tides and longer scale climatic atmospheric and oceanic oscillations). Continued profile
85 monitoring would be required to determine the maintenance of the dynamic equilibrium profile and the
86 response to *SLR*. Thus, while numerous field experiments intended to investigate the applicability of
87 the Bruun Rule have occurred, given the temporal constraints required to capture the development and
88 response of the dynamic equilibrium profile, compromises in experimental design are usually required.

89 For example, instead of mean profiles, instantaneous profiles that feature perturbations such as bars and
90 berms have been used along with proxies for *SLR,* such as rising lake levels (e.g. Hands, 1979), varying
91 tidal ranges (Schwartz, 1967) and land subsidence (Mimura and Nobuoka, 1995). Even in reduced scale
92 laboratories, generating a dynamic equilibrium profile as well as assessing its subsequent response to a
93 slow change in water level would require prohibitively long duration experiments due to the simulation
94 of a variable wave climate of sufficient complexity and duration. However, the qualitative similarity in
95 morphological responses and profile development observed at smaller scales may provide useful
96 insights into natural, prototype profile responses.

97 To date, there has been no published laboratory based experiment on the recession response of
98 the shoreline (or any other vertical datum) to sea level rise. There has only been one laboratory study
99 conducted, in which the Bruun Rule was partially assessed using bar-forming, monochromatic waves
100 in very small scale conditions (Schwartz, 1967). These cases are discussed in more detail in Section 2.
101 Therefore, further investigation into the applicability of the Bruun Rule on beach profiles shaped by
102 wave action is warranted. This paper presents the findings of a recent assessment of the original Bruun
103 Rule, as well as Rosati et al.'s (2013) recent variant, under controlled laboratory conditions at a larger
104 scale than those of Schwartz (1967), and which include both barred and bermed profile responses. A
105 new method for assessing the recession of a profile with a constant change in mean water level is also
106 introduced in the discussion section. Recession of individual contours, such as the still/mean water
107 shoreline can easily be affected by short-temporal fluctuations with different wave conditions and
108 natural bar/berm responses of the beach profiles, introducing noise into the dataset which leads to
109 uncertainty in quantifying the general profile recession. However, if the profile is in a state of dynamic
110 equilibrium, maintained at each water level, and the limits of the profile change are known, the mean
111 recession of all contours in the active profile between the depth of closure and the runup limit, relative
112 to each still water level, should be the recession predicted by Eq. (2). If this is the case, any two
113 instantaneous profiles separated sufficiently in time, can be used to determine the recession due to SLR.
114

115 The paper is organised as follows: Section 2 presents and discusses further background relevant
116 to the present paper and outlines the recent variants to the original Bruun Rule and key issues to be
117 investigated. Methodology follows in Section 3, with descriptions of the experimental setup and
118 analytical techniques, including a description of the new profile translation model applied to different
119 idealised beach profiles. The experimental results are presented and discussed in Section 4 with some
120 general discussion provided in Section 5 and concluding remarks given in Section 6. A companion paper
121 (Beuzen et al., 2017, in review) extends the current work to consider the response of beaches to *SLR* in
122 the presence of structures.

123

124 **2. Background**

125 *2.1 Previous assessments of the* Bruun Rule

126 Schwartz performed very small-scale laboratory experiments in a flume with dimensions 2.3 m
127 length and 1 m width, using fine (0.2mm) sand and small monochromatic waves with heights, H,
128 ranging between 0.005m < H < 0.031m. Qualitative agreement with the Bruun Rule was reported as the
129 profile was observed to rise by values close to the applied rise in water level and shift landward through
130 apparent seaward net-sediment transport. However, the landward recession and net sediment transport
131 were not quantified. Schwartz (1967) also conducted field experiments using neap-spring tides as a
132 proxy for *SLR* and again found qualitative agreement with Bruun Rule predictions, where profiles
133 responded to the increased tidal range with a reduction in beach volume and raising of the offshore
134 profile. However, alongshore migrating sand waves added uncertainty to these findings due to
135 potentially imbalanced longshore sediment transport. Kraus & Larson's (1988) experiment with tide
136 gave shoreline variations of *ca* 4m in response to a tidal range of 1m which is well below the expected
137 Bruun rule 'recession' of approximately 15m (the overall slope being *ca* 1/15). This reduction
138 corresponds to the response time associated with shoreline change that is considerably larger than the
139 tide period (12.25hours).

140

Investigation of the Bruun Rule based on field observations was undertaken by Hands (1979, 1980) on Lake Michigan. Shoreface profiles were monitored during a period of water level rise (approx. 0.08 m/y between 1967 and 1975) and shoreline recession was observed in many places, with erosion maintaining nearshore profile shapes under rising water levels. Rosen (1979) studied shoreline recession and application of the Bruun Rule at Chesapeake Bay, and found the rule to be in good agreement with observed average recession rates. Dubois (1992) questioned the validity of the studies by Rosen (1979) and Hands (1979, 1980) due to profiles being affected by bluff relief, which is the mass movement of sediment down a slip face that can occur in the absence of coastal processes (e.g. wind, waves, and currents). However, Dubois (1992) did find the Bruun Rule to be in good agreement with measured recession for the beach and nearshore in a region at Lake Michigan that was unaffected by bluff relief. Dubois (1992) reported that the slope on the offshore side of the outer bar remained unchanged after a rise in lake level but the nearshore-bar and trough shape was reasonably well maintained and translated upward by comparable quantities to the water level rise and receded landward by the same amount as the shoreline, leading him to conclude that the Bruun Rule may only be applicable in the beach and nearshore zone.

Rapid land subsidence ($\Delta z \approx$ -0.13 m/y between 1960 and 1970) due to ground water extraction has also been used as a proxy for *SLR* by Mimura and Nobuoka (1995) on the Japanese coast, who found predictions from the Bruun Rule to be within the standard deviation of the measured shoreline change after filtering some noisy shoreline data. Unfortunately, because no subaerial profile data (to provide berm height and foreshore slope) were available, the writers used values considered to be typical of the region, so maintenance of profile shape and volumetric continuity was uncertain.

2.2 Recent variants of the Bruun Rule

The original Bruun Rule, Eq. (2), is a special case, where the profile shape is two-dimensional and perfectly maintained relative to the mean water surface, with the shoreline adjoining the subaerial profile at a square-topped, vertical berm. Of course, there could be a scenario where the profile shape

168 is not maintained, yet the Bruun Rule still provides an accurate measure of shoreline recession due to
169 the natural variability and sensitivity of the shoreline to a varying wave climate. However, its simplicity
170 makes it attractive as a predictor for shoreline response to *SLR*, leading to risk of improper use outside
171 the parameter space upon which it was developed (Bruun, 1988; Cooper and Pilkey, 2004). Typical
172 scenarios that should be excluded are: (i) beaches undergoing a dynamic-equilibrium shift, resulting in
173 a changed mean profile slope ($\frac{W}{B+h_*}$), such as with a change in mean wave climate; (ii) beaches where
174 longshore sediment volumes are unbalanced; and (iii) beaches affected by sources/sinks;
175 headlands/inlets; or hard structures (such as non-sandy substrata, cliffs or reefs). These limitations have
176 led to adaptations of the original Bruun Rule, with additional terms to broaden its applicability (e.g.
177 Stive and Wang, 2003; Thorne and Swift, 2009; Rosati et al., 2013; Dean and Houston, 2016).

178 While *SLR* is expected to result in upward and landward profile translation, it may also induce
179 changes in the shape of the active profile and associated sediment transport processes. For example,
180 overwash enhances landward sediment transport across the beach face (Baldock et al., 2008) and
181 induces changes in the sediment budget. To account for this, additional terms may need to be added to
182 the Bruun Rule model. Two such recent contributions are those of Rosati et al. (2013) and Dean and
183 Houston (2016).

184 *Accounting for profile variability above the mean water level*

185 Berms are formed by the deposition and accumulation of sediment near the runup limit and are
186 common features on accretive shorefaces. To maintain the berm shape with profile translation due to
187 *SLR*, the region behind the berm at the initial water level must be filled with sediment, which acts as a
188 sink, increasing the recession needed to maintain a profile relative to the mean water level. Rosati et al.
189 (2013) presented a modified Bruun Rule with an additive term to account for this, the deposition
190 volume, V_D (m^3/m):

$$R = SLR\frac{W + V_D/SLR}{B + h_*} \tag{3}$$

Rosati et al. (2013) note the model is conceptual and acknowledge difficulty in its application in a predictive sense, which requires quantification of the deposition volume. In the field, the subaerial profile is often also dependent on aeolian processes; therefore, overwash is just one of potentially multiple aspects of subaerial shoreface morphodynamics that may affect the recession with profile translation (Davidson-Arnott, 2005; de Vries et al., 2014). Estimates of sediment overwash volume over beach berms is technically feasible (Baldock et al., 2008; Figlus et al., 2010) but not applicable at the timescales associated with profile response to SLR. However, an estimate of deposition volume and recession may be obtained by applying a profile translation model that maintains the subaerial profile shape, assuming a state of equilibrium with the prevailing quasi-steady weather and wave climate (e.g. the new profile translation model introduced later in Section 3.5).

Accounting for other processes resulting in gradual profile variability

Among others, Dean and Houston (2016) provided a Bruun Rule based shoreline change model that included a suite of additional terms. Along with general terms for sediment sources and sinks and alongshore transport gradients, Dean and Houston's (2016) model includes a separate term for sediment introduced from deeper water across an offshore boundary, Φ. This requires an offshore limit that is shallower than that defined by Bruun (1988), i.e., h_* in Eq. (2). Dean and Houston (2016) use an annual closure depth, defined as an estimated depth where, for an average year, "sediment motion was active to a significant degree", which allows for small but significant sediment transport across the boundary, given sufficient time. If the limiting depth of profile change is taken at a longer time-scale (e.g. Bruun 1988) the area of onshore transport may be contained within the active profile and so Φ may not be required as an additional term. Nonetheless, the onshore transport given in Dean and Houston's formula is important in its own right, and is linked to profile steepening described by Rosati et al. (2013). Onshore transport occurring from deeper to shallower regions should act to offset the recession due to *SLR.*

Dean and Houston (2016) suggest calculating Φ at their offshore boundary through application of measured historic data. As suggested by Rosati et al. (2013) and Dean and Houston (2016), to apply

these additional factors an extensive knowledge of the coastal system and processes influencing the sediment transport and budget is required. In an enclosed laboratory flume environment, these additional processes either do not occur or are more easily quantified than in the field. At the time of writing, to the authors' knowledge, there has been no experimental validation of the additional terms presented by Rosati et al. (2013) or Dean and Houston (2016).

2.3 Alternative approaches

The response of beach profiles has been assessed using the original concepts of conservation of the chosen profile shape and volume continuity via simple profile translation models. For example, Cowell et al. (1992; 1995) developed the Shoreface Translation Model (STM) and adopted an active profile shape of the form $h = Ax^m$. In contrast to the implementation of this formula in Eq. (1), the A coefficient and m exponent are adjusted to fit the natural profile being investigated, rather than being defined by physical parameters associated with the region (Cowell et al. 1995). Once determined, the translation maintains the profile shape and operates by volumetric continuity. More recently, Patterson (2013) developed a large-scale translation model also based on volumetric continuity, but differs from the STM by allowing the representative profile to change with time and with sediment transport being process driven. Both of these models use an idealised profile shape that corresponds to the long-term dynamic-equilibrium mean-profile.

The Bruun Rule, in the form of Eq. (2), assumes a vertical berm at the shoreline with a horizontal crest of infinite length (e.g. Figure 1). It is important to note that the entire active profile is being translated, not just the shoreline, and both the subaqueous shoreface and subaerial beach typically deviate from such simply shaped profiles, which may affect the sediment budget (Allison and Schwartz, 1981). Natural beach profiles do not closely follow the 2/3-power profile shape, containing perturbations such as bars, troughs and steps. Others have found compound profiles, introducing a perturbation at the intersection of the two profiles, to more appropriately represent some mean profile shapes (e.g. Inman et al., 1993; Patterson and Nielsen, 2016). Thus, it is important to consider profile shapes that deviate from the monotonic profile of Eq. (1) with respect to net sediment transport

occurring during profile response. Many field investigations of profile response to *SLR* have focused on the shoreline response (Komar et al., 1991). The shoreline is an easily measurable and consequently attractive state parameter, but its definition is subject to different interpretations (Boak and Turner, 2005), which could result in different measures of recession. To better resolve the recession parameter, *R*, it may be useful to consider the entire active profile, given that it is not just the shoreline that recedes. When applying the Bruun Rule to a monotonic profile described by Eq. (1), the shoreline, berm crest and possibly an offshore limit are the only features that are easily distinguishable for measurement of profile recession. Natural profiles, on the other hand, have other features that can be reliably identified, such as bars, troughs and steps. However, these features of the surf zone can be changeable, so their feasibility as reliable state indicators in nature is uncertain and while such features may be transient, the long term mean profile shift, relative to the water surface, should indicate the recession induced by the *SLR;* this is discussed further in Section 5. Subaerial beach profiles are also variable and typically not square-topped like Figure 1, which will affect the recession due to variability in the sediment budget and overtopping accommodation space of the subaerial profile. Therefore, a new translation model that assumes constant profile shape and volumetric conservation, but which uses a measured profile that may contain perturbations will be investigated. The profile translation model, henceforth PTM, has been developed for this purpose, and is presented in Section 3.5.

The remainder of the paper investigates profile responses to rising water levels, using a medium-scale laboratory wave flume. Key issues investigated are: (i) the degree of profile stabilisation under stationary wave conditions and preservation of the stabilised profile shape after a change in water level under the same wave conditions; (ii) cross shore sediment redistribution and the bulk and local net-sediment transport caused by water level changes; (iii) the effects of sediment sources and sinks at both ends of the active profile; (iv) the response of barred and bermed profiles to water level changes; and (v) a laboratory assessment of the original Bruun Rule (Bruun, 1962), the recent variant introduced by Rosati et al (2013) and a simple profile translation model applied to profiles shaped under stationary wave conditions.

3. Methodology

3.1 Wave flumes and instrumentation

Beach profile evolution experiments designed to test the Bruun Rule were performed in a medium scale wave flume at the University of Queensland (UQ). The flume is 20 m long, 1 m wide and operates with a water depth between 0.5 m and 0.8 m (Figure 2). Waves were generated by a piston-type wave maker with active wave absorption enabled. Resistance-type wave gauges were used to measure the offshore waves over the horizontal bed section of the flume.

Selection of initial beach profile

The 2/3 power profile demonstrated by Bruun (1954) and Dean (1973) are clearly reasonable fits to some shoreface mean-profiles; however, opinions vary as to the seaward extent of the 2/3-power profile. Dean's (1977) derivation, using energy dissipation is valid for the breaker region only and some suggest it only extends as far as the surf zone (Larson, 1988; Dette et al., 2002). However, Bruun's (1954) original analysis fitted the 2/3-power law to profiles extending beyond the surf zone, to depths of 15 m. Others have found better fits using compound profile types (e.g. Inman et al., 1993; Patterson and Nielsen, 2016) and natural profiles can also exhibit near-planar mean profiles. For example, Figure 3a shows multiple profiles taken over 1.5 years from the 'ETA63' transect on the Gold Coast, Australia (Patterson, 2013). A linear underlying profile exists between −15 m MSL and mean sea level (approx. 0 m MSL) and Figure 3b demonstrates a smaller mean-error (given in the legend) associated with the planar profile compared with the closest fitting 2/3-power profiles, calculated by varying the A parameter ($0.14 \leq A \leq 0.19$) in Eq. (1). Interestingly, some of the best-fit profiles in Dean's (1977) study were also best represented by linear profiles, where $m = 0$ in Eq. (1).

At small scales, beach profiles tend to be steeper (Vellinga, 1982), and it is the experience of the authors that a 1:10 profile evolves under the available wave conditions to produce both barred and bermed profile types. Planar starting slopes are useful when trying to achieve comparable starting conditions between different tests so most of the profiles were initially shaped to a 1:10 planar slope

and topped by a wide berm above the runup limit at the back of the beach. However, to investigate potential differences obtained using a planar and concave initial profile, one experiment (E-3) used a monotonic power-law profile, shaped according to the form of Eq. (1). The scaling parameter, A, was determined by the offshore limit of water depth at the flume bed, h_0 = 0.6 m, and the sandy profile width from the shoreline to the bed, set at x_{sl} = 8 m, to provide (Riazi and Turker, 2017) $A = h_0(x_{sl})^{-2/3} = 0.15$ m$^{1/3}$. This is in good general agreement with the expected values of A based on the grain size (Dean, 1977). To avoid a vertical sloped berm at the shoreline, a 1:10 planar profile was tangentially connected to the monotonic profile (Kriebel and Dean, 1993). The profiles developed at each water level from both the planar and power-law profiles exhibited a good degree of similarity in profile shape and recession (more detail of the two profile responses are provided in Section 4). Profiles were allowed to progress toward equilibrium, so the actual starting profile for the response to water level change is no longer planar, but a profile at equilibrium with the wave climate.

There remains a further practical consideration for choosing a plane initial or underlying profile, linked to the choice of depth of closure or the limiting depth used to define W and h_* in Eq. (2). There is some uncertainty in the measurement of the limiting depth but, provided this location is chosen to be offshore of the true limit, any error in that choice is cancelled out in Eq. (2) with planar profiles. This is not the case for non-planar profiles. For example, if the offshore limit is chosen further offshore than the true limit on a profile where the depth varies as $x^{2/3}$, the overall beach gradient will be measured as milder than the true gradient, and application of the Bruun Rule would result in an overestimated prediction of the recession and *vice versa*. A planar profile is unbiased in this respect for model-data comparisons of Eq. (2). Profiles were comprised of natural marine beach sand, $d_{50} \approx 0.28$ mm. Closure errors in volumetric sediment transport calculations may occur if the sand in the flume is not compacted sufficiently; in these experiments the sand had been exposed to hundreds of hours of waves prior to the initial tests. When resetting the planar profile, the redistributed sediment was carefully compacted

manually through the entire profile. Thus, only minor compaction closure errors are expected during the first few profile measurements after wave exposure.

Early testing found that alongshore non-uniformity may occur in the 1m wide flume, particularly with monochromatic and accretionary waves, complicating investigation of cross-shore two-dimensional sediment transport processes. This was found to be mitigated by the addition of two thin (2 mm) brass plates orientated cross-shore, dividing the upper shoreface and beach into three equal-width compartments. These dividers extended typically from above the run-up limit into the mid-surf zone and are self-supporting, inserted vertically into the sand to a sufficient depth to remain buried during the experiment.

The laboratory beach profiles were measured using a non-contact laser profiler capable of measuring both the subaqueous and subaerial profiles from above the water surface with no bed disturbance and no requirement to drain the flume or change water levels (Atkinson and Baldock, 2016). Data is obtained at a resolution of 1 mm in both the vertical and horizontal and the accuracy is of order ±2 mm and capable of resolving bed ripples and beach scarps. The profiler comprises eight lasers mounted across the flume on a trolley, aligned to capture multiple cross-shore profiles along the flume simultaneously by traversing the trolley horizontally along the length of the flume (Figure 2). The mean profile from all eight lasers was used for all calculations and model comparisons.

3.2 Wave and water level conditions

Various researchers have attempted to produce empirical formulae to predict beach response to different wave conditions (e.g. Gourlay, 1968; Sunamura and Horikawa, 1974; Hattori and Kawamatta, 1980); however, there is uncertainty when using any empirical formulae outside of the parameter space in which it is developed, and many of the predictive formula are developed for use in the field or with monochromatic waves. Therefore, wave conditions for the present experiments were chosen through

347 experience gained from previous experiments, where distinct barred or bermed profiles were observed
348 to develop under known conditions (Baldock et al., 2017).

349 An overview of the experimental program is provided in Table 1. A total of six experiments were
350 conducted, comprising three barred profiles and three bermed profiles. In each case, wave conditions
351 were held constant to allow the beach to progress toward a stable profile, at which point the water level
352 was changed and the waves resumed. In a companion paper, Beuzen et al. (2017, in review) conducted
353 experiments investigating the difference in profile development under a single step water level rise and
354 multiple, incremental steps, to the same level as the single step. Although the intermediate profile
355 development differed, the shoreline recession and beach profile at the end of each experiment were near
356 identical, irrespective of the water level progression. The Bruun Rule, Eq. (2) itself is also independent
357 of the rate of *SLR*. Therefore, due to time restrictions on operators, for experimental simplicity and
358 expediency, the experiments detailed in this paper applied a single step change in water level. Beach
359 profiles were frequently measured during profile development at each water level to assess progression
360 toward a stable state. For all but experiment A-1, the total change in water level corresponded to half
361 the incident significant wave height (H_{sig}), representing the ratio given by a likely forecast *SLR* of order
362 0.5 m over the remainder of the century (RCP 8.5, IPCC 2013) relative to an annual mean wave height
363 (on the Australian East coast) of order 1 m. Of course, the experiments presented here have stationary
364 wave climates, so the profile response cannot be expected to respond as it does in the field with a variety
365 of wave conditions and varying water levels, influencing the profile at various depths, however, given
366 the requirement to choose a constant water level change, this ratio seems as appropriate as any.
367
368 Using monochromatic waves to generate barred profiles tends to develop cross-tank non-
369 uniformity after very long run times since the constant breakpoint at the bar tends to result in positive
370 feedback if the bar skews. Initially, monochromatic wave experiments were conducted and found this
371 to be the case, therefore, due to the high likelihood of profile instability with monochromatic waves on
372 barred profiles, only random wave experiments were conducted for the barred profile experiments. The
373 barred profile experiments consisted of three random wave experiments with similar wave conditions,

E-1, E-2 and E-3. Note, experiments E-1 and E-1C are the same experiment, with different durations following the water level rise due to a cyclic morphodynamic response that occurred. Waves at the initial water level were run for 49 hours for experiment E-1/E-1C to allow sufficient time for profile development and stabilisation. Experiment E-1C (C for cyclic) contains the full dataset where profile development continued for 393 hours after water level rise where three cycles of bar generation and decay were observed. Given the added complexity introduced by the cyclic bar behaviour and disproportionate run time between the two water levels, an additional analysis on the same data set (experiment E-1, Table 1) was performed using the initial portion of the dataset, enabling comparison of the profiles at similar run times at each water level. To avoid a cyclic response during experiment E-2 and E-3, the test durations were limited to 50 hours at each water level.

Three experiments investigating bermed profile responses to water level changes were conducted, consisting of two monochromatic wave experiments with weak (A-1) and strong (A-2) accretion, and one random wave experiment (A-3, Table 1). Experiment A-1 was conducted as a pilot study prior to the installation of the laser profiling system and profiles were measured by surveying the profile at discrete intervals with a horizontal spatial resolution of 0.25 m ±5 mm, and a vertical accuracy of approximately ±5 mm.

3.3. Sediment transport calculations

Considering the framework presented by Bruun (1988), it is apparent that along with measuring spatial variations of profile parameters (e.g. the location of the shoreline, bar or berm) to assess recession values, the mode and direction of sediment transport is also important. Obtaining high resolution profile data allows increased confidence in the calculation of sediment transport rates through volumetric conservation (e.g. Exner, 1925; Pelnard-Considere, 1956):

$$\frac{\delta q_s}{\delta x} \approx -(1-p)\delta z \tag{4}$$

where q_s is the net sediment transport (i.e., the volume moved through a cross-section per unit width, with units m^2, positive onshore), δx is the horizontal (cross shore) increment (m), p is the sediment porosity (taken as $p \approx 0.4$ for sand), and δz is the change in bed elevation (m). Note, usually there is a time component associated with q_s, we have omitted this as a variable since at equilibrium the duration of the experiment becomes irrelevant.

The local cross shore net sediment transport per unit width, $q_s(x)$, is calculated through integration of Eq. (4) over the active profile domain between the limiting depth ($h_* = x_{min}$) and the berm height (or runup limit) above the still water level ($B = x_{max}$), corresponding to the most landward location of observable profile change, to provide:

$$q_s(x) = (1-p)\int_x^{x_{max}} \delta z \, \mathrm{d}x \tag{5}$$

While minimised with high spatial-resolution measurements, closure errors (q_s (x_{min}) $\neq 0$, where the integration commences from the landward limit, x_{max}, seaward) in the integration can still occur with unaccounted volume missed due to the alongshore spatial separation of the lasers, variable porosity, or compaction due to wave action. Closure errors are dealt with following the methodology of Baldock *et al.* (2011) by uniformly distributing the residual error through the active profile between x_{min} and x_{max}. Plotted against x, the output of Eq. (5) highlights areas where volumetric imbalances may be required to be considered for implementation of the additional term in Eq. (3), for example, see Section 3.4 and Figure 4c, where berm overwash generates a region of net-onshore transport.

A second useful beach profile change and transport parameter, following Baldock et al. (2011), is the bulk sediment transport, Q_s (m^3 per unit width) which is determined by integration of Eq. (5):

$$Q_s = \int_{-\infty}^{\infty} q_s\,(x)\mathrm{d}x \tag{6}$$

where positive (or negative) Q_s represents a net shoreward ($Q_s > 0$) or seaward ($Q_s < 0$) motion of the sediment volume that comprises the active profile, which has been used to classify the overall profile response as erosive ($Q_s < 0$), accretive ($Q_s > 0$) or stable ($Q_s \approx 0$) (Baldock et al., 2011; Jacobsen and

421 Fredsoe, 2014). Q_s is also equivalent to the horizontal change of the first moment of the beach profile
422 and does not equal zero unless the onshore and offshore magnitudes of $q_s(x)$ are equal. Therefore, Q_s
423 provides an integrated measure of the overall redistribution of sediment, providing the direction by its
424 sign, relative to the coordinate system. Relative to a given, earlier profile, Q_s evolves to a constant value,
425 as the profile progresses toward equilibrium (cf. Jacobsen and Fredsoe, 2014).
426
427 *3.4 Model assessment*
428 Three models were assessed for their accuracy in predicting the observed shoreline recession. The
429 original Bruun Rule (Bruun, 1962) was assessed by measuring the shoreline recession for each
430 experiment and comparing with the prediction by selecting the profile limits where the profile change
431 is consistently less than the measurement accuracy of the profiling technique.
432 The recent modification of Rosati et al. (2013) was tested in the same way as the Bruun Rule, with
433 the additional step of measuring and applying any deposition volume, V_D, determined by the net
434 sediment transport (calculated between the initial and final profile at the raised water level) that occurs
435 at the berm crest of the initial profile, x_{berm}, and re-introducing the porosity:

$$V_D = \frac{q_s(x_{berm})}{1-p} \tag{7}$$

436 Finally, a new profile translation model was assessed by comparing the translated initial water level
437 profile and the measured raised water level profile and respective net-sediment transport curves. The
438 profile translation model will now be described further.
439
440 *3.5Profile Translation Model*
441 As proposed in the Section 2.3, a new geometric translation model may help to investigate the
442 response of natural profiles (that may contain perturbations) to sea level rise. This section details the
443 method of the profile translation model (PTM). The PTM initially raises the active profile by the water
444 level rise, connecting to the original profile at each end with a vertical line. At this point the volumes
445 are not conserved between the initial and translated profile, so the raised profile is incrementally shifted

landward, always connected by vertical lines to the original profile, until the volumes balance. Volumetric continuity is determined by integration of the translated and original profiles. The PTM was tested by applying to some idealised profile shapes, with net transport distributions also calculated. Figure 4a shows the classic example of the Bruun Rule with a monotonic 2/3-power profile and vertical berm at the shoreline. This example confirms model behaviour in accordance with the Bruun Rule: only offshore sediment transport is present, and the new profile is offset in the landward direction. The sediment from the upper profile facilitates raising the offshore profile, and the recession predicted by Eq. (2) agrees to within 1% of the value obtained from the PTM. The slight discrepancy is due to the finite resolution of the model (profile interpolated at δx = 1 mm increments). During the incremental horizontal shift, the algorithm stops at the first instance the volume balance crosses zero, producing a slightly greater value than that of Eq. (2).

Figure 4 also shows three other scenarios (b, c and d). Figure 4b shows the translation applied to a shoreface with a sloping upper beach face instead of a vertical berm, the net sediment transport curve again indicates offshore transport only. The recession predicted by the Bruun Rule and PTM are again near identical, and are greater than the vertical berm scenario, corresponding to a milder active profile slope. Figure 4c shows the translation applied to the same idealised profile as 4b, but with a berm inserted onto the beach. In this case onshore transport occurs, leaving a deposition volume landward of the original berm. Figure 4d shows the PTM applied to one of the ETA63 Gold Coast profiles (Patterson and Nielsen, 2016) that features a large offshore bar. Both examples containing a perturbation (Figure 4c and 4d) generate localised net onshore transport (indicated by the $q_s(x)$ curve) following the translation, near the perturbation.

Note that the profile translation for the idealised case with the berm (Figure 4c) generates more recession than the case without the berm (Figure 4b), which agrees with the concepts of Rosati et al. (2013). Applying the Bruun Rule, Eq. (1), to the bermed profile in Figure 4c, and taking the landward extent for the profile width, W, as the coordinates at the berm crest yields:

471 $$R = SLR\frac{W}{B + h_*} = 0.41 \text{ m}$$

472 whereas the PTM predicts a recession of 0.48 m (Figure 4c). Calculating the deposition volume using
473 Eq. (7) ($q_s(x_{berm}) = 0.024$, as indicated in Figure 4c) gives $V_D \approx 0.040$ m^2 and inserting into Rosati et al.
474 (2013)'s Eq. (3) gives:

475 $$R = SLR\frac{W + V_D/SLR}{B + h_*} = 0.48 \text{ m}$$

476 this agrees with the PTM. These results indicate that the deposition volume requirement may be
477 predicted using a translation model, and that the predictions from the PTM automatically include the
478 deposition volume of Rosati et al. (2013) where it occurs.

479

480 *3.6 Scaling*

481 Scale effects are expected in reduced scale physical models (Vellinga, 1982). However, beach
482 evolution in similar sized laboratory conditions to those in the present study have been compared with
483 that of much larger scale facilities (Baldock *et al.*, 2011) and found to have exhibited quantitatively
484 comparable patterns in sediment transport rates for erosive and accretive conditions. Experiments at
485 both scales also exhibited features that are typical of natural beaches, e.g. formation of scarps, beach
486 berms, beach steps, breaker bars and troughs. All these features of beach profiles are observed in the
487 present experiments and therefore the physical model reproduces the classical morphodynamic
488 responses observed in the field. Additionally, Van Rijn (2011) compared profile development in
489 laboratories over three different scales and found the shoreline recession to be in good quantitative
490 agreement between all three scales; however due to finer sand in the smallest scale, the offshore profile
491 was smoother. The coarser sediment used in the present experiments would be less likely to suffer this
492 effect so may generate more realistic subaqueous profile shapes. However, the use of sediment size
493 similar to that of prototype conditions would result in a distortion between horizontal and vertical scales
494 (Vellinga, 1982), typically producing steeper profiles at smaller scales.

495

The principles of the Bruun Rule, geometric similarity and conservation of volume remain true at laboratory scale. Considering the inevitability of scale effects on local sediment transport, the aim of the present experiments was to ensure similitude in profile responses. That is, to generate barred or bermed profiles with similar morphological evolution to that observed in the field. While the present experiments do not attempt to model any specific beach, the profiles do respond with sufficient similarity to natural beaches, considering the distortions introduced by the sediment scaling limitations. For example, taking the barred profile experiment significant wave heights, H_s = 0.13 m and considering that typical annual average significant wave heights on the Gold Coast, Australia, (which commonly feature bars, Figure 3) are of the order $H_s \approx 1$ m, a vertical length scale ratio of $N_{Lvertical} \approx$ 8-10 may be reasonable. Froude scaling, requires the fall velocity of the sediment to scale with the square root of the length scale, such that $N_{ws} = N_{Lvertical}^{0.5} \approx 3$, which would correspond to a prototype grain size of around 0.8 mm, which is typical on natural beaches with gradients of 1/10 (e.g. Weir et al., 2006). Conversely, using $\frac{H\beta_{sz}}{w_s T}$ (where w_s is the sediment fall velocity and β_{sz} is the surf zone slope) as a similarity parameter (Hattori and Kawamata, 1980) indicates that if the grainsize does not change between the prototype and the model, the 1/10 planar initial slope represents a prototype beach with a gradient approximately three times smaller. Beaches with slopes of 1/30 typically generate longshore bars during intermediate and erosive events as observed in the present experiments.

Therefore, given that reduced-scale laboratory profiles: (i) behave with sufficient similarity to barred and bermed profile responses observed in nature; (ii) respond at reduced time scales; (iii) profile responses can be quantified with more accuracy and confidence in the absence of longshore processes; and (iv) are more financially feasible and accessible; it is considered appropriate to be assessing the qualitative aspects of the beach responses to changing water levels at the scales presented. Therefore, physical modelling to investigate beach response induced by raised water levels is warranted.

3.7 Determining profile stabilisation or equilibrium attainment

Wave conditions in the present research are held constant (stationary for random waves) with no tidal or seasonal variability so profiles were expected to progress toward a stable *equilibrium* state that contain perturbations in the form of bars and troughs or berms and steps. Equilibrium is expected to develop at an exponentially decaying rate of change (Sunamura, 1983), which could result in prohibitively long experiment durations, and may not hold after certain durations due to oscillations about some near-equilibrium state. Even in medium scale wave flumes, a true equilibrium may be unattainable in any reasonable length of time, if at all (cf. Swart, 1974 figures 16, 43 or 44). Therefore, in the present experiments, determining profile stabilization and/or attainment of equilibrium was assessed on a case by case basis. The profile development was monitored through changes in state parameters, such as the location of the shoreline, bar and berm crest, as well as considering sediment transport rates and broad profile changes. Once the profile was deemed to have stabilised sufficiently the water level change was implemented and profile development toward a new stable state commenced. As shown in Figure 5, the shoreline and bar crest locations were observed to stabilise over time. The net and bulk transport rates often did not reach a zero value, which would be expected if a true equilibrium profile had occurred. Instead small near-constant rates corresponding to small changes in profile shape were common long after the shoreline, bar crest and/or step and berm locations had stabilised; and in these instances, the active profile was also considered to have stabilised sufficiently to change the water level. For simplicity, we refer to these as profiles at equilibrium, noting the above caveats. A cyclic process of bar generation and decay was observed in experiment E-1C, after a run time of approximately 100 hours, after which the definitions of equilibrium become invalid. This cyclic bar behavior is consistent with observations from other studies (Swart, 1974 figures 43 and 44) and is discussed further below. Hence, a subjective decision was required to cease a run when a sufficiently stable profile is achieved prior to the possible triggering of a cyclic mode of evolution.

4. Results

This section presents and discusses the results of the experiments. Table 2 provides all onshore and offshore limits, measured values for the deposition volume, V_D, in equation (3), and the measured

549 and predicted shoreline recession for each model. Figure 6 shows each predicted recession value against
550 the observed shoreline recession for each experiment and Figure 7 provides the percentage error
551 $(error(\%) = 100\left(\frac{R_{predicted}}{R_{observed}} - 1\right))$ of each model with respect to the observed shoreline recession for
552 each experiment.

553 The results are presented as follows. First, the cyclic bar morphodynamic response, following the
554 water level rise in experiment E-1C will be presented (Figure 8). Following this, the analysis focuses
555 on barred and bermed profile response (Figures 9-13). Figures 9-13 each contain four plots (a, b, c and
556 d). (a) shows the profile development for both the initial and raised water levels. Note, t = 0 indicates
557 the time the water level was raised. Therefore, in these figures, there are two shoreline locations shown
558 at t = 0 h, corresponding to the final shoreline location at the initial water level and the new shoreline
559 location at the raised water level. (b) gives the cumulative bulk sediment transport and relative
560 shoreline progression (relative to the initial shoreline location at the start of the experiment). (c) shows
561 the initial and final equilibrium profiles at each water level, as well as the results of the PTM. (d)
562 provides the local net transport distributions ($q_s(x)$) between the initial water level equilibrium profile
563 and the raised water level equilibrium profile and translated profile. The period at the initial water level
564 prior to water level rise are indicated by negative time values along the abscissa.
565
566 *4.1 Barred profile experiments*
567 Experiments E-1C, E-1, E-2 and E-3 were conducted to investigate barred profile responses to increased
568 water levels when forced with random waves.
569
570 *Cyclic bar with random waves E-1C*
571 Figure 8a shows the profile development during the cyclic morphodynamic response at the raised
572 water level over 393 hours. Figure 8b provides the cumulative bulk sediment transport and relative
573 shoreline progression (relative to the initial shoreline location at t = 0 h). The cyclic profile response at
574 the raised water level resulted in sustained losses of sediment offshore, resulting in a gradually receding

shoreline, the location of which was under predicted by all three of the tested models (Table 2, Figure 6 and Figure 7). At $t \approx 65$ h the bar, having been stable for around 30 hours, progressively decayed over 14 hours and the inner bar grew and propagated offshore (Figure 8a). This cyclic bar behaviour was captured three times before the experiment finished and is discussed further in Section 6. An investigation into the offshore wave conditions throughout the experiment confirmed that they were consistent. The shoreline exhibits progradation at certain times, which appear to align with the initial stages of bar stabilisation. The cumulative bulk transport demonstrates periods of stability ($dQ_{s,cumulative}/dt \approx 0$) and accretion ($dQ_{s,cumulative}/dt > 0$) within an overall erosive trend ($dQ_{s,cumulative}/dt < 0$). The accretion events appear to occur around times when the bar either stabilises or decays, with the strongest accretion occurring at the end of the experiment during bar decay.

Figure 8c and Figure 8d detail two different profile responses and the net sediment transport. The left plots show the profile response between 70 h $< t <$ 77 h when the bar was decaying rapidly. A strong net-onshore transport component occurs ($x \approx 11$ m) as most of the sediment from the bar fills in the trough, although there is also small offshore transport further seaward, corresponding to the gradual offshore accumulation. The right plots show the profile response between 107 h $< t <$ 114 h when the inner bar was rapidly migrating offshore; at this time, there is almost no onshore transport component.

Common responses of the barred profile experiments

At the initial water level ($t < 0$ h, Figure 9a and 10a), the bar grows quickly by eroding the initial profile around the shoreline and nearshore (approx. 11 m $< x <$ 13 m) and both the bar and shoreline stabilise by $t \approx -20$ h, although a gradual continued offshore movement of sand is typically indicated by the cumulative Q_s plot at the end of the initial water level and slight shoreline recession is still occurring (Figure 9b and 10b). However, given the relative stability compared with changes occurring between -50 h $< t < -20$ h, the experiments continued with water level rises at this point. Other recent experiments (Baldock et al., 2017) also found that even with very long run times there may be a small degree of net sediment motion landward or seaward despite single state profile parameters (e.g. shoreline and bar crest elevation) appearing stable.

Following the water level change, only small (of order of the measurement accuracy) changes were observed in the profile elevation offshore of the initial bar crest following water level rise, which agrees with Dubois' (1992) field observations. The PTM tended to predict a lowered profile offshore of the original bar (Figure 9c and 10c) and onshore transport in the region of the bar (Figure 9d and 10d), which exhibits qualitative similarity with the translated Gold Coast profile (Figure 4d). However, this onshore transport was not observed in the experimental data for experiments E-1 and E-2, although E-3 did exhibit a small amount of net-onshore transport in the bar region. The shape of the final profiles through the surf zone was often markedly different at the different water levels. The landward translation of the bar crest was typically less than that of the shoreline, indicating wider surf zones at the raised water levels, although the crest elevation of the main breaker bar typically translated vertically by a comparable value to the water level change. Shoreward of the inner bar, the measured and PTM predicted cross-shore transport patterns, $q_s(x)$, were in good agreement, with the additional observed recession reflected by the greater amount of offshore transport ($q_s(x) < 0$) throughout the upper profile for experiments E-2 and E-3. While the surf zone profiles remained changeable, profile similarity was reasonably maintained on the beach face (Figure 9c and 10c) and the shorelines tended to stabilise for $t > 30$ h (Figure 9b and 10b). Thus, after the initial response to the change in water level and the shoreline receding due to erosion, little further sediment is required from the upper profile. Instead, the surf zone sediment is gradually redistributed, which does not significantly influence the shoreline location during the remaining evolution. For all three barred profile experiments there were only slight differences between the original Bruun and Rosati et al. (2013) model predictions (Table 2, Figure 6 and Figure 7), due to none or only a small quantity of sand deposited above the still water level.

Experiment E-1

All variants of the Bruun Rule and the PTM predicted the shoreline recession to within 6% (Table 2 and Figure 7). Figure 9 shows the results for experiment E-1. The rate of change for Q_s also tends to zero by the end of the experiment ($t = 44$ h and 51 h). The change in trend for Q_s around $t = 30$ h, and the slight accretive shoreline response, may indicate stabilisation of the overall system. The minor

629 progradation of the shoreline once the new bar had fully developed may be a result of the evolution of
630 the inner bar, leading to a reduction in wave energy at the shore. There was only a single bar in the final
631 profile of the initial water level. At the raised water level, a double bar and step profile remained at
632 $t = 51$ h and the main breaker bar and trough (10 m < x < 11.5 m) were more defined than those at the
633 initial water level (Figure 9c), with the result that the initial profile shape was not exactly conserved
634 following the water level increase.
635
636 *Experiment E-2*
637 The original Bruun Rule and Rosati et al.'s (2013) modified version provided slightly closer
638 predictions than the PTM, but the difference was minimal and all models under predicted the recession
639 by approximately 25% (Table 2 and Figure 7). Figure 10b-d illustrate the results of the second erosion
640 experiment, E-2, where the time at each water level was limited to 50 hours. The profile stabilised at
641 the initial water level around $t \approx -20$ h with a well-defined two-bar profile, which was a similar
642 evolution time to Experiment E-1. After the water level rise, continued offshore transport resulted in a
643 recession that was much greater than the model predictions, with errors that were comparable with the
644 experiment E-1C (Figures 6 and 7).
645
646 *Experiment E-3*
647 After water level rise, a small amount of deposition above the shoreline resulted in minor
648 differences between the original Bruun Rule and Rosati et al.'s (2013) modified version, which both
649 underpredicted the observed shore recession by approximately 13%. The PTM had a slightly greater
650 underprediction of 16% (Table 2 and Figure 7). Figure 10a-d also details the results of the erosion
651 experiment where the initial profile was shaped to a monotonic, concave-up profile. Comparably with
652 experiment E-2, the profile stabilises at the initial water level around $t \approx -20$ h with a well-defined two-
653 bar profile (dash-dot blue line, Figure 10c). The cumulative bulk sediment transport appears to have
654 stabilised to a greater degree than the planar case for this initial profile.
655

656 *4.2 Bermed profile experiments (A-1 to A-3)*

657 Profile stability under monochromatic waves on bermed profiles was achieved using the channel
658 dividers, therefore regular and random wave experiments are presented. Experiments A-1, A-2 were
659 forced by monochromatic waves and A-3 was forced by random waves (Table 1).

660

661 *Experiment A-1*

662 Figure 11 provides the results of experiment A-1, which resulted in a mild accretive response,
663 building a small berm through onshore transport of sediment. Rapid profile development and
664 stabilisation is apparent from the contour plot and plots of the cumulative bulk sediment transport and
665 relative shoreline position. Due to the low measurement resolution, the calculations of the deposition
666 volume and the assessment of profile similarity are subject to greater error than for other experiments.
667 However, the shoreline position was measured accurately. With reference to Figure 6, Figure 7 and
668 Table 2, the original Bruun Rule under-predicted the shoreline recession by 23%, the Rosati et al. (2013)
669 model under-predicted shoreline recession by 14%, and the PTM provided the best prediction, with an
670 under-prediction of 11%. The net sediment transport curve in Figure 11d displays a qualitatively similar
671 shape to the measured data in the nearshore, but there are deviations further offshore which may be due
672 to the development of periodic bars, commonly generated by standing waves which are stationary with
673 monochromatic wave conditions. The predicted deposition volume from the PTM was $V_D = 0.027$ m^3/m,
674 which is greater than that observed, and would further improve the predictions of Rosati et al. (2013).
675 There appears to be a slightly wider berm formed at the initial water level and a more pronounced step
676 in the final raised water level profile, which may account for some of the discrepancies.

677

678 *Experiment A-2*

679 Experiment A-2 ran larger waves with a longer period (Table 1) to promote a stronger accretive
680 response than for Experiment A-1. Figure 12 illustrates the results, where a large, well defined berm
681 was built by the waves through onshore transport of sediment. The contour plot, temporal variation in
682 the cumulative Q_s, and the shoreline position all indicate profile stabilisation and a trend towards

683 equilibrium. The original Bruun Rule under-predicted the shoreline recession by 7%, while the other
684 models overestimate the recession. Using the measured V_D (Eq. (7)), the Rosati et al. (2013) model, Eq.
685 (3), overestimated the observed recession by 7% and the PTM overestimated by 15% (Table 2, Figure
686 6 and Figure 7). The predicted deposition volume from the PTM was $V_D = 0.039$ m^3/m, which is greater
687 than that observed (Table 2), consistent with the overestimated recession. Much of the translated profile
688 receded by more than the measured profile but there is a very close similarity between the profiles before
689 and after the water level rise (Figure 12c). The measured and modelled net sediment transport curves
690 are in reasonable agreement (Figure 12d), but the magnitudes for the PTM are greater, consistent with
691 the overestimated recession.
692
693 *Experiment A-3*
694 Figure 13 provides the results for the random wave experiment, A-3. The shoreline stabilised for
695 a period before the water level rise at $t = 0$ h, but then began accreting slowly around $t \approx -10$ h, because
696 of the berm's continued (albeit very slow) growth seaward. Following the raised water level, the
697 cumulative Q_s curve and shoreline both stabilise, indicating near equilibrium conditions at the raised
698 water level from approximately $t > 30$h, with very similar values at $t \approx 16$ h also. There is also a gradual
699 loss to offshore deposition, leading to a deeper offshore limit, following the raised water level.
700 The net sediment transport, q_s (x), curves between the initial and raised water level profiles show
701 a greater amount of transport occurring in both directions compared with the translated PTM profile,
702 corresponding to an increasing berm volume as well as greater losses of sediment offshore, resulting in
703 the profile lowering around $x \approx 11$ m. Although there was a substantial onshore transport associated
704 with the deposition volume, all models over-predicted the shoreline recession (Table 2, Figure 6 and
705 Figure 7). Due to the deposition volume, the predicted recession by Rosati et al. (2013) (+27%) was
706 greater than that of the original Bruun Rule (+10%) and the PTM (+17%). The predicted deposition
707 volume from the PTM was $V_D = 0.017$m^2, half of that observed (Table 2). We propose two possible
708 reasons for this. Firstly, the profile may not have progressed far enough toward equilibrium by the time
709 the water level was changed. However, the profile appeared to have stabilised sufficiently by the usual

710 measures (shoreline, step and berm crest locations). Secondly, overtopping enhances landward sediment
711 transport by reducing the backwash (Baldock et al., 2008) and therefore the presence of the berm at the
712 outset of the test at the raised water level promotes greater onshore transport than that which would
713 have occurred on the plane beach. Therefore, exact profile similarity cannot be expected since the
714 hydrodynamic-morphodynamic feedback is different in the two tests and this factor is expected to be
715 exacerbated by the random waves, with variable runup limits. This additional transport occurs in the
716 inner surf zone (11 m < x < 12 m), and while allowing the berm to grow, also feeds the subaerial beach
717 profile, resulting in less recession than predicted.
718
719 **5. Discussion**
720 From the experiments presented, it is clear that the morphodynamic processes leading to profile
721 change under rising water levels are extremely complex. Even in reduced scale, and with simplified and
722 controlled laboratory settings, interactions between the hydrodynamics and morphodynamics of mobile
723 beds results in variable profile responses that can be strongly influenced by many factors. These factors
724 include, but are not limited to: the rate of water level fluctuations, feedback mechanisms in the near
725 shore, the presence of berms under random waves, standing waves due to wave reflection, the
726 underlying/initial profile slope, and wave-boundary interactions. Following the step change in water
727 level, the initial and intermediate response and development of the profiles to reattain equilibrium are
728 not representative of a profile developing with a gradual *SLR*. The actual response to SLR on natural
729 beaches is also far more gradual with many other higher-frequency fluctuations occurring at the same
730 time. Features like the discontinuity in the PTM figures are not present when the water level changes
731 are gradual, essentially infinitesimal, which may produce the trailing ramp proposed by Kriebel and
732 Dean (1993). However, as proposed in Sections 1 - 3, the assumptions underpinning the Bruun Rule
733 should remain valid for any rate of water level rise, and at any scale. Given the evidence that the final
734 profile at equilibrium does not depend on the rate of water level change (Beuzen et al.., 2017, in review),
735 we assume the final profiles obtained following a step water level rise do represent the *SLR* response.
736

737 The cyclic behaviour observed in E-1C may be due to a slow offshore transport of sediment,
738 indicated by the offshore accumulation between 8 m < x < 10 m (Figure 8). The bar crest elevations
739 gradually decrease (Figure 14) until the proportion of breaking waves is no longer sufficient to maintain
740 the bar, triggering the decay (e.g. Wijnberg, 1997). Gradual deepening of the bar crest appears to be a
741 common occurrence and has also been documented in prototype scale laboratory experiments (Kraus
742 and Larson, 1988). Baldock et al. (2017) have linked this trigger to the orbital wave velocity over the
743 bar crest progressively reducing, until the threshold for sheet flow on the bar crest is no longer
744 maintained. Ripples then form, leading to diffusion of sediment away from the bar crest. Note that this
745 may not always be the case; bars have also been observed to migrate to a new location with varying
746 water levels while maintaining their form (e.g. Nielsen & Shimamoto, 2015).
747 The profile response with initially planar starting conditions and a classical concave power-law
748 profile is very similar (Figure 10c), as are the derived sediment transport distributions. Slightly greater
749 offshore transport is present for the planar profile case (E-2). This may be due to a greater requirement
750 for sediment to build the offshore flank of the bar, particularly at the initial water level for the planar
751 initial condition, and/or decreased wave energy dissipation seaward of the bar over the steeper offshore
752 slope (x < 9 m), which may also be the cause of the slightly deeper offshore bar crests for Experiment
753 E-2. Nevertheless, there is good similarity between the profiles at equilibrium for the two experiments
754 at each water level, providing similar net-transport distribution patterns, as well as very close agreement
755 in terms of the shoreline recession, which differs by less than 2% (R_{shore}, Table 2). The difference in the
756 predicted shoreline recession for E-3 and E-2 are greater than the measured differences, which
757 highlights the uncertainty introduced when choosing the limiting depth on the non-planar slope.
758
759 *5.1 Mean recession of the profile*
760 While the shoreline change models generally underestimate the shoreline recession, the use of a
761 single beach state parameter to assess the Bruun rule is only robust if the profile shape is conserved
762 exactly, i.e. small changes in profile shape due to, e.g., bar/berm responses around the waterline will
763 lead to differences between measurement and predictions even if the overall profile recedes as predicted.

764 To address this issue a global measure of the recession of the profile would be useful. To some extent
765 this is provided by the PTM model. However, the PTM still assumes conservation of the profile shape.
766 We therefore determine the mean recession, R_m, of the profile by averaging the recession of the profile
767 at discrete, individual contours, R (z), between the offshore and onshore limits of profile change

768 $$R_m = \overline{R(z)} = \frac{1}{z_B - z_{h*}} \int_{-\infty}^{\infty} \{\overline{x_{t1}(z + SLR)} - \overline{x_{t0}(z)}\} \mathrm{d}z$$

769 where subscript $t1$ and $t0$ indicates two profiles separated in time. Thus, for varying water levels, the
770 contours for each profile are defined relative to the respective still water levels, i.e., the water level
771 change (SLR) is accounted for. To demonstrate, Figure 15a shows the same translated 2/3-power profile
772 response to SLR as that in Figure 4a. Figure 15b shows the $R(z)$ aligned with the initial water level
773 profile. In this example, all contour recessions, the Bruun Rule, the PTM prediction and R_m are all equal,
774 because of the profile shape maintenance.

775 Figure 16 shows the result of applying this analysis to the final profiles at each water level of
776 Experiment E-1C, where the shoreline recession at the end of the experiment was much greater as a
777 result of the cyclic bar response and continued offshore transport. Figure 16a shows the two profiles
778 with bars, but quite different profile shapes through the surf zone. To better visualise the profile
779 recession the elevations of the profile at the raised water level were reduced by the water level change
780 (0.065 m) to vertically align with the final profile at the initial water level. Figure 16b shows $R(z)$, along
781 with vertical lines that indicate the mean contour recession, R_m, the Bruun Rule prediction, the PTM
782 prediction and the measured shoreline recession, R_{shore}. Note that, now the profile shape is not conserved
783 at each water level, $R(z)$ is variable. This is particularly noticeable around elevations -0.21 m $< z < 0$ m.
784 $R(z)$ is greater than R_m above the shoreline (approximately 0.8 m), highly variable around the bar, and
785 offshore of the bar $R(z)$ is less than R_m.

786 R_m is close to the recession predicted by the PTM and when the profile shape is exactly conserved
787 relative to the still water level the two are equal, e.g. Figure 15. Therefore, a difference between the
788 PTM prediction and R_m gives an indication of experimental error. Sources of experimental error may
789 be due to lack of equilibration (at either water level), compaction issues, cross-tank non-uniformity, or

790 measurement error. Figure 17 shows the percentage error of each model's predicted recession with
791 respect to R_m, for each experiment, where a negative percentage error indicates an under prediction of
792 the model compared with R_m. In comparison with Figure 7, the performance remains variable, but the
793 absolute error is reduced in most cases. Exceptions are Experiment E-1, where the predictions remained
794 similar, and the Bruun Rule predictions for Experiments A-2 and A-3. The models under predicted R_m
795 in many cases; a possible reason for this would be if the profiles had not progressed far enough toward
796 equilibrium at the initial water level. Using the percentage error of the PTM to indicate experimental
797 uncertainty suggests that both the Bruun (1962) and Rosati et al. (2013) models provided predictions
798 that were within 5% of the observations for the erosion experiments, accounting for experimental errors.
799 The predictions from the model of Rosati et al. (2013) were within the expected experimental
800 uncertainty. Therefore, the inclusion of the overtopping volume improved the prediction, accounting
801 for the sediment that was transported landward. This is particularly evident for the bermed profile
802 experiments, where overtopping was more influential.
803 Using a single measure of the profile recession, such as the shoreline or any other contour relative
804 to the different still water levels, introduces error and is sensitive to profile shape. The mean recession
805 of the profile, calculated from many contours through the active profile, provides a more robust
806 measurement of the mean profile response to changes in water level and does not require the profile
807 shape to be maintained. This method may be applicable to field profiles also, assuming the field profile
808 can be assumed to be two dimensional (e.g., no longshore net sediment transport gradients). Under these
809 conditions, conservation of volume requires that the mean recession of the profile in response to a
810 change in water level should equal the recession of the dynamic-equilibrium mean profile. Therefore,
811 any two profiles may be used to calculate the mean recession, providing the limits of the active profile
812 due to cross-shore processes are known. Similar methods may be applicable for other applications, such
813 as determining longshore transport gradients.
814
815 The additional term in the shoreline change model of Dean and Houston (2016) described in
816 Section 2.2, Φ, which quantifies the volume of sediment introduced into the active profile from seaward

817 of the depth of closure, could not be assessed in the present experiments. In order for there to be a
818 notional shallower limiting depth, such as the annual limit of change, a non-stationary wave climate is
819 required to produce variable profiles. This will be investigated in a later paper where further experiments
820 with falling and rising water levels and a wave climate that cycles between erosive and accretive
821 conditions are considered, along with the results of nourishment experiments.

822

823 **6. Conclusions**

824 The accuracy of the Bruun Rule (Bruun, 1962), Rosati et al.'s (2013) recent variant and a new
825 profile translation model (PTM) has been assessed using measured profile changes to different water
826 levels in medium scale laboratory wave flumes. Experiments were performed for both random wave
827 and monochromatic wave conditions to form barred and bermed profiles. Beach profile data with high
828 spatial and temporal resolution were obtained using a laser profiler capable of measuring the sub-
829 aqueous profile from above the water surface, from which sediment transport rates were derived.

830 The comparison of observed and predicted recession values show that as a measure of shoreline
831 response to rising water levels the original Bruun Rule predicted the shoreline recession to within 25%
832 (generally under predicting the observations). Rosati et al.'s (2013) Bruun Rule variant exhibited a slight
833 improvement when the original Bruun Rule under predicted the observations, but resulted in greater
834 error in some other cases. The PTM was developed to work on measured profiles, accounting for
835 overwash deposition automatically and performed comparably with the empirical formulas of Bruun
836 (1962) and Rosati et al. (2013). The recession of discrete contours was calculated across the active
837 profile to provide a global measure of the mean recession of the profile, and this value was in better
838 agreement with the recession predicted by all three models, with errors typically reducing to the order
839 of 10%.

840

841 **Acknowledgements**

842 The authors gratefully acknowledge support from the Australian Research Council through an
843 APA award to Alexander Atkinson and through Discovery grant DP140101302.
844 Roshanka Ranasinghe is supported by the AXA Research fund and the Deltares Harbour, Coastal
845 and Offshore engineering Research Programme 'Bouwen aan de Kust'.
846
847 **References**
848 Allison, H. and Schwartz, M.L. 1981. The Bruun Rule–The relationship of Sea-Level Change to Coastal
849 Erosion and Deposition. *Proceedings Royal Society Victoria*, 93, pp.87-97.
850 Atkinson, A. and Baldock, T.E. 2016. A high-resolution sub-aerial and sub-aqueous laser based
851 laboratory beach profile measurement system. *Coastal Engineering*, 107, 28-33.
852 Baldock, T.E., Weir, F. and Hughes, M.G. 2008. Morphodynamic evolution of a coastal lagoon entrance
853 during swash overwash. *Geomorphology*, 95(3), pp.398-411.
854 Baldock, T. E., Alsina, J. A., Caceres, I., Vicinanza, D., Contestabile, P., Power, H. & Sanchez-Arcilla,
855 A. 2011. Large-scale experiments on beach profile evolution and surf and swash zone sediment
856 transport induced by long waves, wave groups and random waves. *Coastal Engineering,* 58**,**
857 214-227.
858 Baldock, T. E., Birrien, F., Atkinson, A., Shimamoto, T., Wu, S., Callaghan, D.P., Nielsen, P. 2017.
859 Hysteresis in the evolution of equilibrium beach profiles under sequences of wave climates -
860 Part 1; Observations. In review.
861 Beuzen, T., Turner, I. L., Blenkinsopp, C. E., Atkinson, A. L., Baldock, T. E., Flocard, F. 2017. Physical
862 model study of beach profile evolution by sea level rise in the presence of seawalls. *Submitted*
863 *for review – this issue*.
864 Boak, E.H. and Turner, I.L., 2005. Shoreline definition and detection: a review. *Journal of coastal*
865 *research*, pp.688-703.
866 Bruun, P. 1954. Coast erosion and the development of beach profiles, Beach Erosion Board Corps of
867 Engineers.

868 Bruun, P. 1962. Sea-level rise as a cause of shore erosion. *Journal of the Waterways and Harbors*
869 *Division*. Proceedings of the American Society of Civil Engineers. Pp.117-130.
870 Bruun, P. 1988. The Bruun Rule of erosion by sea-level rise: a discussion on large-scale two-and three-
871 dimensional usages. *Journal of Coastal Research*, pp.627-648.
872 Cooper & Pilkey. 2004. Sea-level rise and shoreline retreat: time to abandon the Bruun Rule. *Global*
873 *and Planetary Change*, 43, 157-171.
874 Cowell, P. J., Roy, P. S. & Jones, R. A. 1992. Shoreface translation model: computer simulation of
875 coastal-sand-body response to sea level rise. *Mathematics and computers in simulation*, 33, 603-
876 608.
877 Cowell, P. J., Roy, P. S. & Jones, R. A. 1995. Simulation of large-scale coastal change using a
878 morphological behaviour model. *Marine Geology*, 126, 45-61.
879 Davidson-Arnott, R.G. 2005. Conceptual model of the effects of sea level rise on sandy coasts. *Journal*
880 *of Coastal Research*, pp.1166-1172.
881 de Vries, S., Arens, S.M., de Schipper, M.A. and Ranasinghe, R. 2014. Aeolian sediment transport on
882 a beach with a varying sediment supply. *Aeolian Research*, 15, pp.235-244.
883 Dean, R.G., 1977. Equilibrium beach profiles: US Atlantic and Gulf coasts. Department of Civil
884 Engineering and College of Marine Studies, University of Delaware.
885 Dean, R.G., 1991. Equilibrium beach profiles: characteristics and applications. Journal of coastal
886 research, pp.53-84.
887 Dean, R. G. & Houston, J. R. 2016. Determining shoreline response to sea level rise. *Coastal*
888 *Engineering,* 114**,** 1-8.
889 Dette, H. H., Larson, M., Murphy, J., Newe, J., Peters, K., Reniers, A., Steezel, H., 2002. Application
890 of prototype flume tests for beach nourishment assessment. Coastal Engineering 47. p.137−177
891 Dubois, R. N. 1992. A Re-Evaluation of Bruun's Rule and Supporting Evidence. *Journal of Coastal*
892 *Research,* 8**,** 618-628.
893 Exner, F.M., 1925. Uber die wechselwirkung zwischen wasser und geschiebe in flussen. Akad. Wiss.
894 Wien Math. Naturwiss. Klasse, 134(2a), pp.165-204.

Figlus, J., Kobayashi, N., Gralher, C. and Iranzo, V. 2010. Wave overtopping and overwash of dunes. *Journal of Waterway, Port, Coastal, and Ocean Engineering*, 137(1), pp.26-33.

Hands, E. B. 1979. Changes in Rates of Shore Retreat, Lake Michigan, 1967-1976. DTIC Document.

Hands, E. B. 1980. Prediction of Shore Retreat and Nearshore Profile Adjustments to Rising Water Levels on the Great Lakes. DTIC Document.

Hallermeier, R. J. 1981. A profile zonation for seasonal sand beaches from wave climate. *Coastal Engineering*, 4, 253-277.

Hattori, M. and Kawamata, R., 1980. Onshore-offshore transport and beach profile change. In Coastal Engineering 1980 (pp. 1175-1193).

Hay, C.C., Morrow, E., Kopp, R.E. and Mitrovica, J.X. 2015. Probabilistic reanalysis of twentieth-century sea-level rise. *Nature*, 517(7535), pp.481-484.

Hughes, S.A. 1993. Physical models and laboratory techniques in coastal engineering (Vol. 7). World Scientific.

Inman, D.L., Elwany, M.H. and Jenkins, S.A. 1993. Shorerise and bar-berm profiles on ocean beaches. Scripps Institution of Oceanography.

IPCC. 2013: Summary for Policymakers. In: Climate Change 2013: The Physical Science Basis. Contribution of Working Group I to the Fifth Assessment Report of the Intergovernmental Panel on Climate Change [Stocker, T.F., D. Qin, G.-K. Plattner, M. Tignor, S.K. Allen, J. Boschung, A. Nauels, Y. Xia, V. Bex and P.M. Midgley (eds.)]. Cambridge University Press, Cambridge, United Kingdom and New York, NY, USA.

Jacobsen, N. & Fredsoe, J. 2014. Cross-Shore Redistribution of Nourished Sand near a Breaker Bar. *Journal of Waterway, Port, Coastal, and Ocean Engineering,* 140**,** 125-134.

Komar, P.D., Lanfredi, N., Baba, M., Dean, R.G., Dyer, K., Healy, T., Ibe, A.C., Terwindt, J.H.J. and Thom, B.G. 1991. The response of beaches to sea-level changes-a review of predictive models. *Journal of Coastal Research*, 7(3), pp.895-921.

Kraus, N.C. and Larson, M. 1988. Beach profile change measured in the tank for large waves 1956-1957 and 1962 (No. CERC-88-6). Coastal Engineering Research Center Vicksburg MS

922 Kriebel, D.L. and Dean, R.G., 1993. Convolution method for time-dependent beach-profile response.
923 Journal of Waterway, Port, Coastal, and Ocean Engineering, 119(2), pp.204-226.
924 Larson, M., 1988. Quantification of beach profile change. PhD. Thesis, Lund University (Sweden) Dept.
925 of water resources engineering.
926 Leatherman, S.P., Zhang, K. and Douglas, B.C. 2000. Sea level rise shown to drive coastal erosion. Eos,
927 Transactions *American Geophysical Union*, 81(6), pp.55-57.
928 Ludka, B.C., Guza, R.T., O'Reilly, W.C. and Yates, M.L. 2015. Field evidence of beach profile
929 evolution toward equilibrium. *Journal of Geophysical Research*: *Oceans*, 120(11), pp.7574-
930 7597.
931 Mimura, N. & Nobuoka, H. 1995. Verification of the Bruun Rule for the estimation of shoreline retreat
932 caused by sea-level rise. *Coastal Dynamics 95*. ASCE, 607-616.
933 Nielsen, P. and Shimamoto, T. 2015. Bar response to tides under regular waves. *Coastal Engineering*,
934 106, pp.1-3.
935 Patterson, D. C. 2013. Modelling as an aid to understand the evolution of Australia's central east coast
936 in response to late Pleistocene-Holocene and future sea level change. PhD, University of
937 Queensland.
938 Patterson, D. & Nielsen, P. 2016. Depth, bed slope and wave climate dependence of long term average
939 sand transport across the lower shoreface. *Coastal Engineering*, 117, 113-125.
940 Pelnard-Considere, R., 1956. Essai de theorie de l'evolution des formes de rivage en plages de sable et
941 de galets. Les Energies de la Mer: Compte Rendu Des Quatriemes Journees de L'hydraulique,
942 Paris 13, 14 and 15 Juin 1956; Question III, rapport 1, 74-1-10.
943 Riazi, A. and Türker, U., 2017. Equilibrium beach profiles: erosion and accretion balanced approach.
944 Water and Environment Journal.
945 Rosati, J., Dean, R. & Walton, T. 2013. The Modified Bruun Rule Extended for Landward Transport.
946 *Marine Geology,* 340**,** 71-81.

947 Rosen, P. 1979. An application of the Bruun Rule in the Chesapeake Bay. Proceedings of the Per Bruun
948 Symposium. International Geographical Union, Commission on the Coastal Environment, 1979.
949 Newport, RI, USA, 55-62.
950 Schwartz, M. L. 1967. The Bruun theory of sea-level rise as a cause of shore erosion. *The Journal of*
951 *Geology*, 76-92.
952 Short, A.D. 1999. Handbook of beach and shoreface morphodynamics. John Wiley & Sons.
953 Stive, M. J. F. & Wang, Z. B. 2003. Chapter 13, Morphodynamic modeling of tidal basins and coastal
954 inlets. Elsevier B.V.
955 Sunamura, T. 1983. A predictive model for shoreline changes on natural beaches caused by storm and
956 post-storm waves, *Transactions, Japanese Geomorphological Union*, Vol.4, 1, 1-10.
957 Swart, D.H. 1974. Offshore sediment transport and equilibrium beach profiles (Doctoral dissertation,
958 TU Delft, Delft University of Technology).
959 Thorne, J. & Swift, D. 2009. Sedimentation on continental margins, II: application of the regime
960 concept. *Shelf Sand and Sandstone Bodies. Oxford: Blackwell*, 33-58.
961 Van Rijn, L.C., Tonnon, P.K., Sánchez-Arcilla, A., Cáceres, I. and Grüne, J. 2011. Scaling laws for
962 beach and dune erosion processes. *Coastal Engineering*, 58(7), pp.623-636.
963 Vellinga, P. 1982. Beach and dune erosion during storm surges. *Coastal Engineering*, 6(4), pp.361-387.
964 Wijnberg, K.M. 1996. On the systematic offshore decay of breaker bars. *Coastal Engineering 1996*,
965 3600-3613.

966 Tables

967 **Table 1: Summary of experiments detailing Experiment type, ID, profile type (barred or bermed), significant wave height (H_{sig}), peak wave period (T_p), water level rise (SLR) and**
968 **total run times at each water level. Under Profile type M indicates monochromatic waves P is a Pierson-Moskowitz wave spectrum and J is a Jonswap spectrum (gamma = 3.3). * denotes**
969 **regular wave height, H, and constant period, T, for the monochromatic wave cases, instead of H_{sig} and T_p.**

Experiment	ID	Profile type	H_{sig}	T_p	SLR	Time at initial water level	Time at raised water level
			(m)	(s)	(m)	(h)	(h)
Cyclic Bar	E-1C	Bar (P)	0.13	1.20	0.065	49	393
Barred/Erosion	E-1	Bar (P)	0.13	1.20	0.065	49	56
Barred/Erosion	E-2	Bar (J)	0.13	1.20	0.065	50	50
Barred/Erosion	E-3	Bar (J)	0.13	1.20	0.065	54	50
Weak Accretion	A-1	Berm (M)	0.06*	1.50*	0.050	12	12
Strong Accretion	A-2	Berm (M)	0.07*	2.00*	0.035	12	12
Random Accretion	A-3	Berm (P)	0.10	2.00	0.035	41	40

970

Table 2: ID, Bruun Rule parameters (*SLR*, h_*, *B* and *W*), observed shoreline recession (*Rshore*), observed mean contour recession (*Rm*) and recession predictions, *R*, for the original Bruun Rule (Bruun), the translation model (PTM), and Rosati et al.'s (2013) model (R13). Percentage error (*%Error*) is provided next to each model's prediction compared with the observed, depicted in Figure 9.

				Bruun						PTM		R13		
ID	***SLR***	***Rshore***	R_m	h_*	*B*	*W*	β	*R*	*%Error*	*R*	*%Error*	V_D	*R*	*%Error*
[-]	[m]	[m]	[m]	[m]	[m]	[m]	[-]	[m]	[%]	[m]	[%]	[m^3/m]	[m]	[%]
E-1C	0.065	0.869	0.758	-0.575	0.094	6.803	0.098	0.661	-23.9	0.689	-20.7	0.0007	0.662	-23.8
E-1	0.065	0.696	0.706	-0.575	0.094	6.803	0.098	0.661	-5.0	0.689	-1.0	0.0017	0.664	-4.7
E-2	0.065	0.883	0.698	-0.495	0.100	6.087	0.098	0.665	-24.7	0.663	-24.9	0.0005	0.666	-24.6
E-3	0.065	0.870	0.750	-0.409	0.092	5.830	0.086	0.756	-13.1	0.731	-16.0	0.0000	0.756	-13.1
A-1	0.05	0.553	0.522	-0.383	0.045	3.651	0.117	0.427	-22.9	0.490	-11.4	0.0202	0.474	-14.3
A-2	0.035	0.312	0.328	-0.476	0.148	5.191	0.120	0.291	-6.7	0.358	14.7	0.0273	0.335	7.3
A-3	0.035	0.307	0.381	-0.462	0.162	5.999	0.104	0.336	9.6	0.360	17.3	0.0341	0.391	27.4

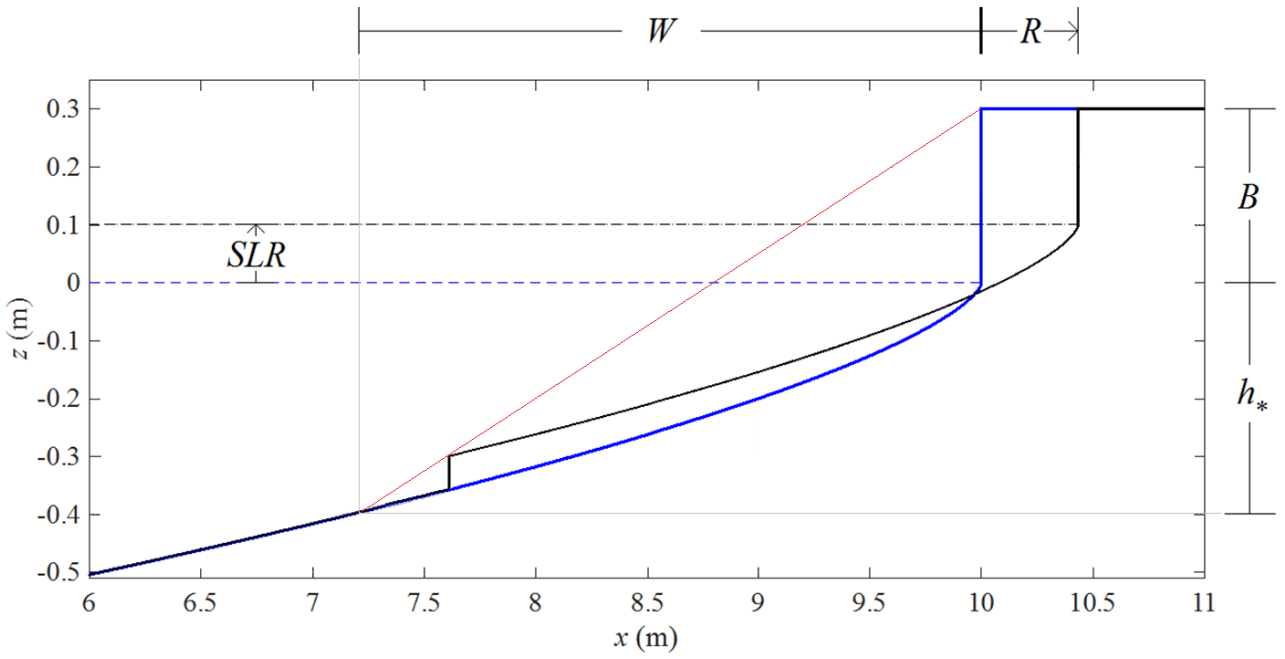

Figure 1: Bruun rule profile response and framework applied to an idealised profile with offshore shape corresponding to Eq. (1). The red line indicates the slope of the dynamic equilibrium active profile, between the offshore limit and berm crest. The z-axis origin is at the initial water level (blue line), the x-axis origin is located off the plot, seaward of the offshore limit of the profile at the initial water level $(x, z) = (7.2\text{ m}, -0.4\text{ m})$.

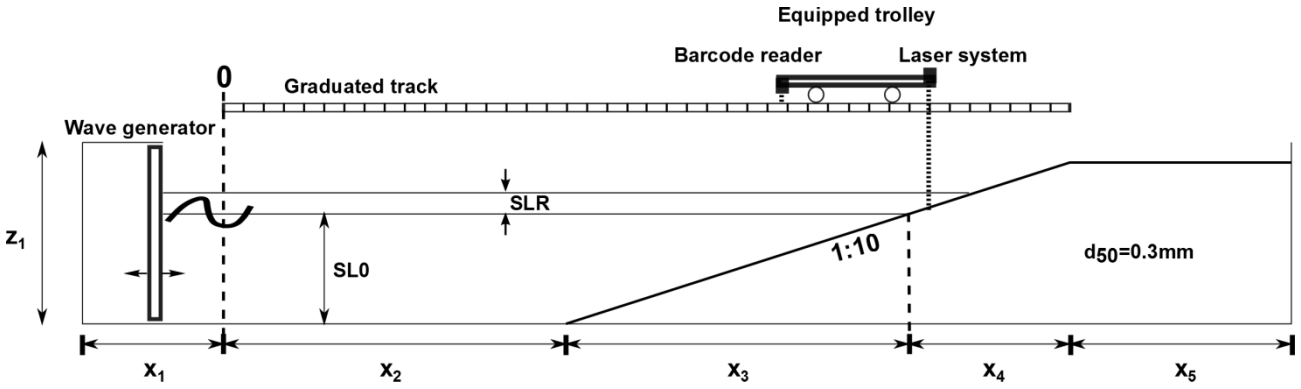

Figure 2: Wave flume and instrumentation schematic ($x_1 \approx 3$ m; $x_2 \approx 7$ m; $x_3 \approx 6$ m; $x_4 \approx 2$ m; $x_5 \approx 2$ m; $z_1 = 1$ m).

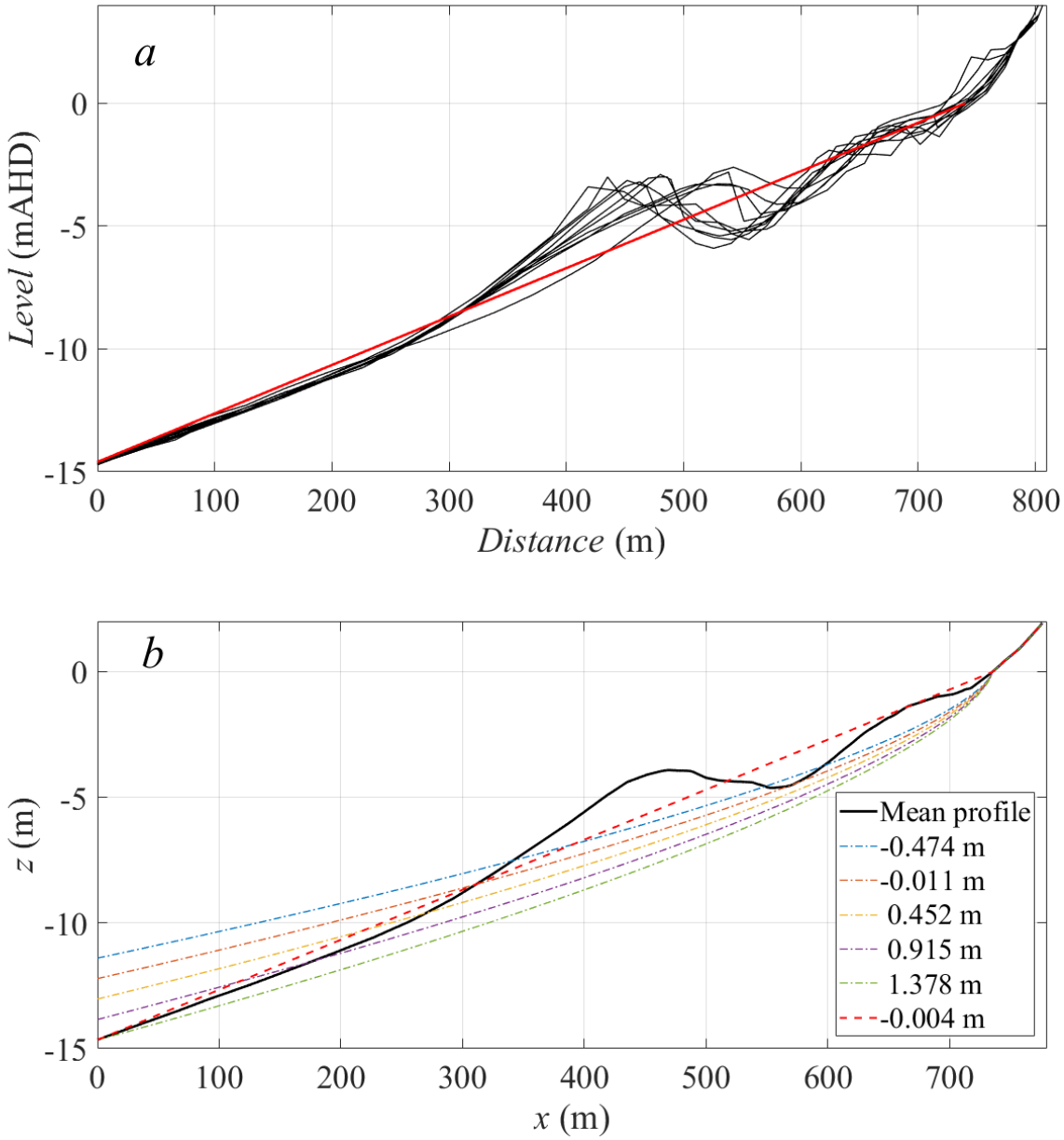

Figure 3: a) Profiles of a beach at the Gold Coast, Australia (ETA 63) with multiple measurements taken over approximately 1.5 years, with best fit planar profile shown in red. b) 2/3 power law profiles plotted for a range of A values ($0.14 \leq A \leq 0.18$) together with the planar profile, red, and the mean of the measured profiles (black). The legend shows the mean error of the vertical difference between the mean profile and the idealised profiles. Profile data from Patterson (2013)

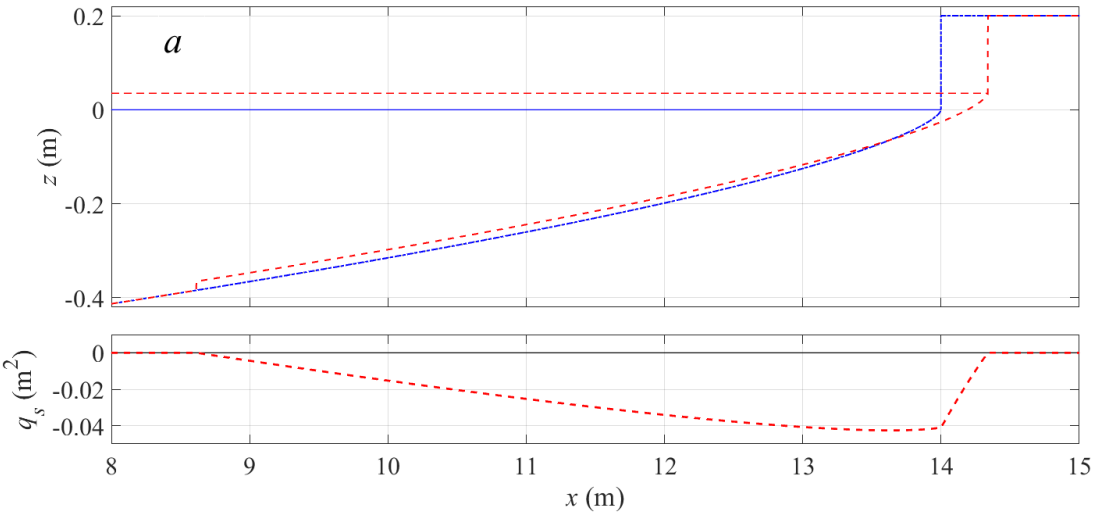
a
0.2
0
-0.2
-0.4
z (m)
0
-0.02
-0.04
q_s (m^2)
8
9
10
11
12
13
14
15
x (m)

996

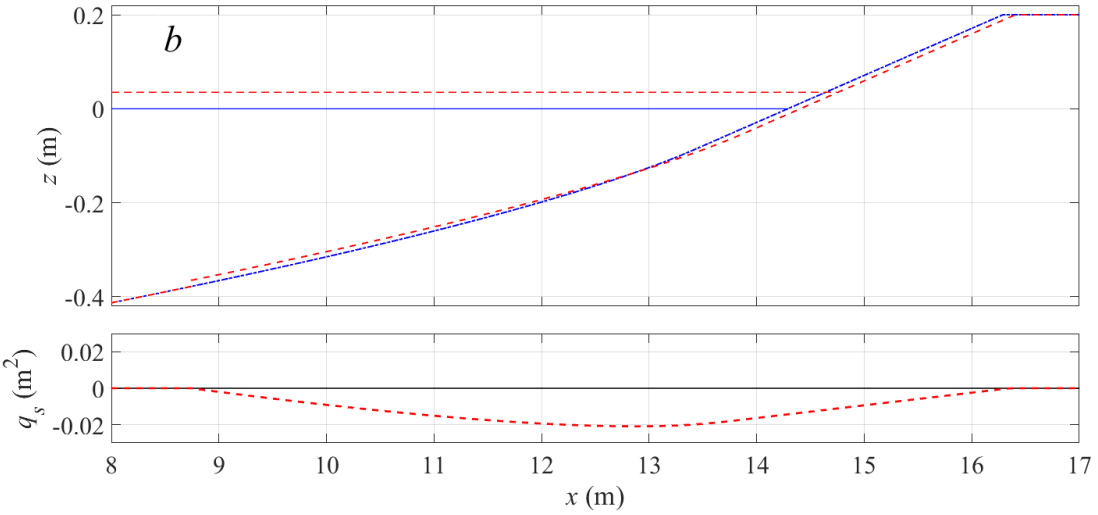
b
0.2
0
-0.2
-0.4
z (m)
0.02
0
-0.02
q_s (m^2)
8
9
10
11
12
13
14
15
16
17
x (m)

997

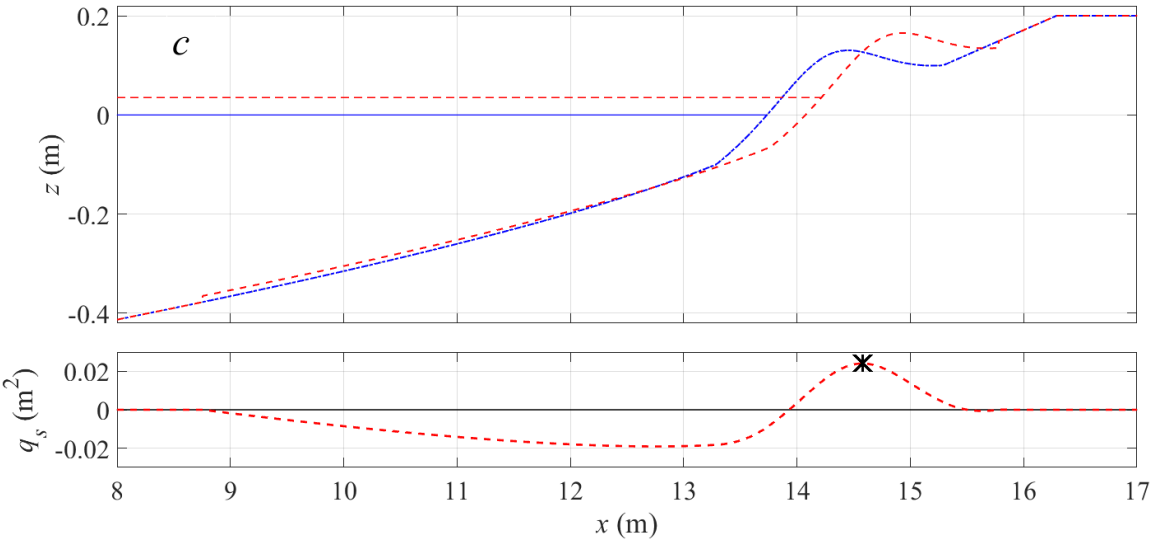

998

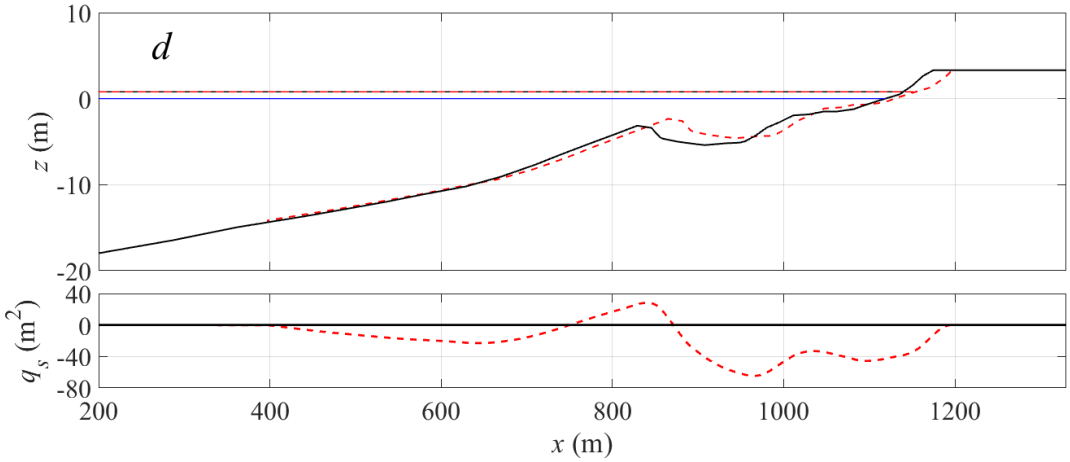

999

1000 Figure 4: Profile Translation Model results (top panels) and corresponding net-sediment transport
1001 curves (offshore transport when $q_s < 0$) in the lower panels for: a) classical Bruun-type power-law
1002 profile; b) power-law profile spliced to a plane sloping upper beach (cf. Kriebel and Dean, 1993); c)
1003 power-law profile with berm on upper beach (note the black star on the $q_s(x)$ plot indicates the net-
1004 sediment overtopping, $q_s(x_{berm}) = 0.024$ m^2); and d) ETA63 Dec 1988 Gold Coast Profile with the berm
1005 crest extrapolated landward.

1006

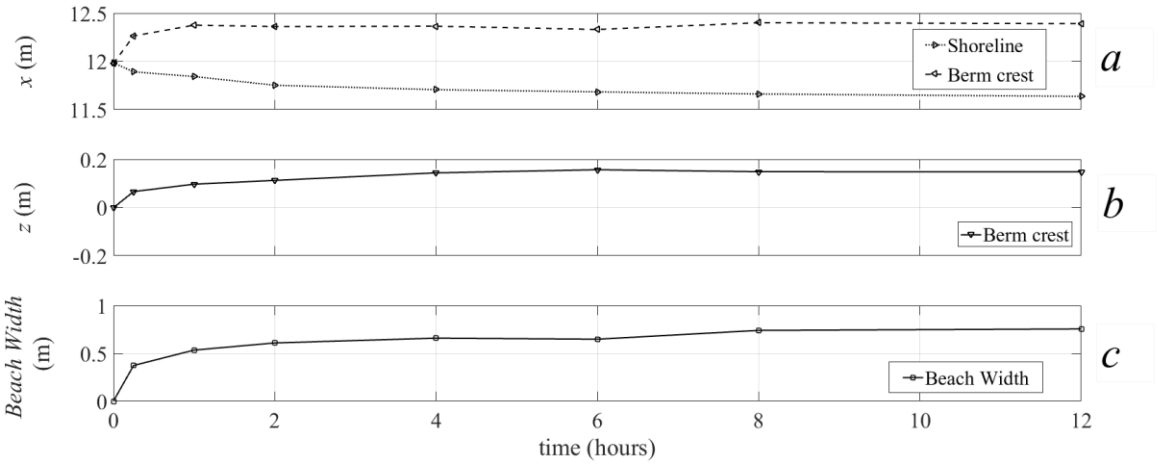

Figure 5: Evolution of profile parameters over time for experiment A-2. a) Shoreline and berm crest horizontal coordinate location, b) berm crest elevation and c) beach width (x_{berm} - $x_{shoreline}$).

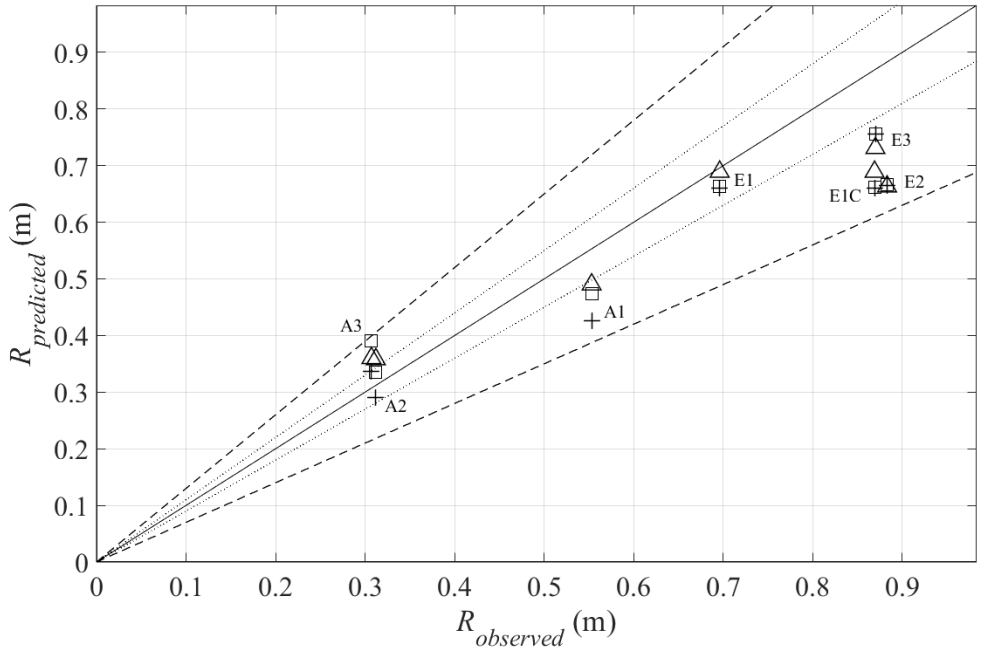

Figure 6: Predicted versus observed recession of the shoreline for all experiments. Models predictions are identified by different markers: Original Bruun Rule (+), PTM (triangles) and Rosati et al.'s (2013) variant (squares). Solid, dotted and dashed lines indicate 0%, ±10% and ±30% error bounds, respectively.

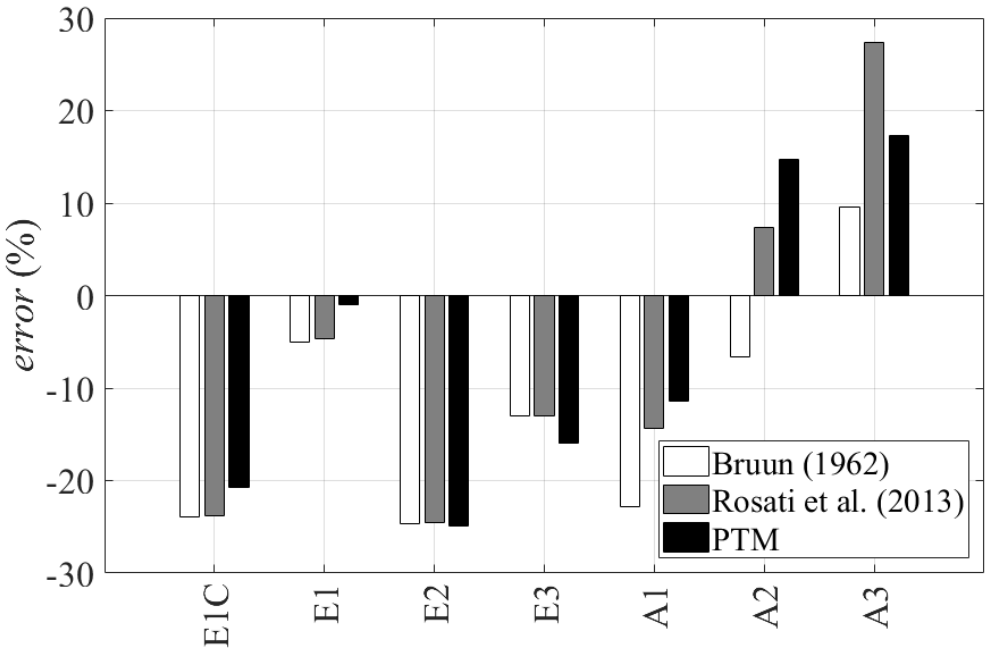

Figure 7: Percentage error of each model with respect to the observed recession. Positive values indicate an over prediction.

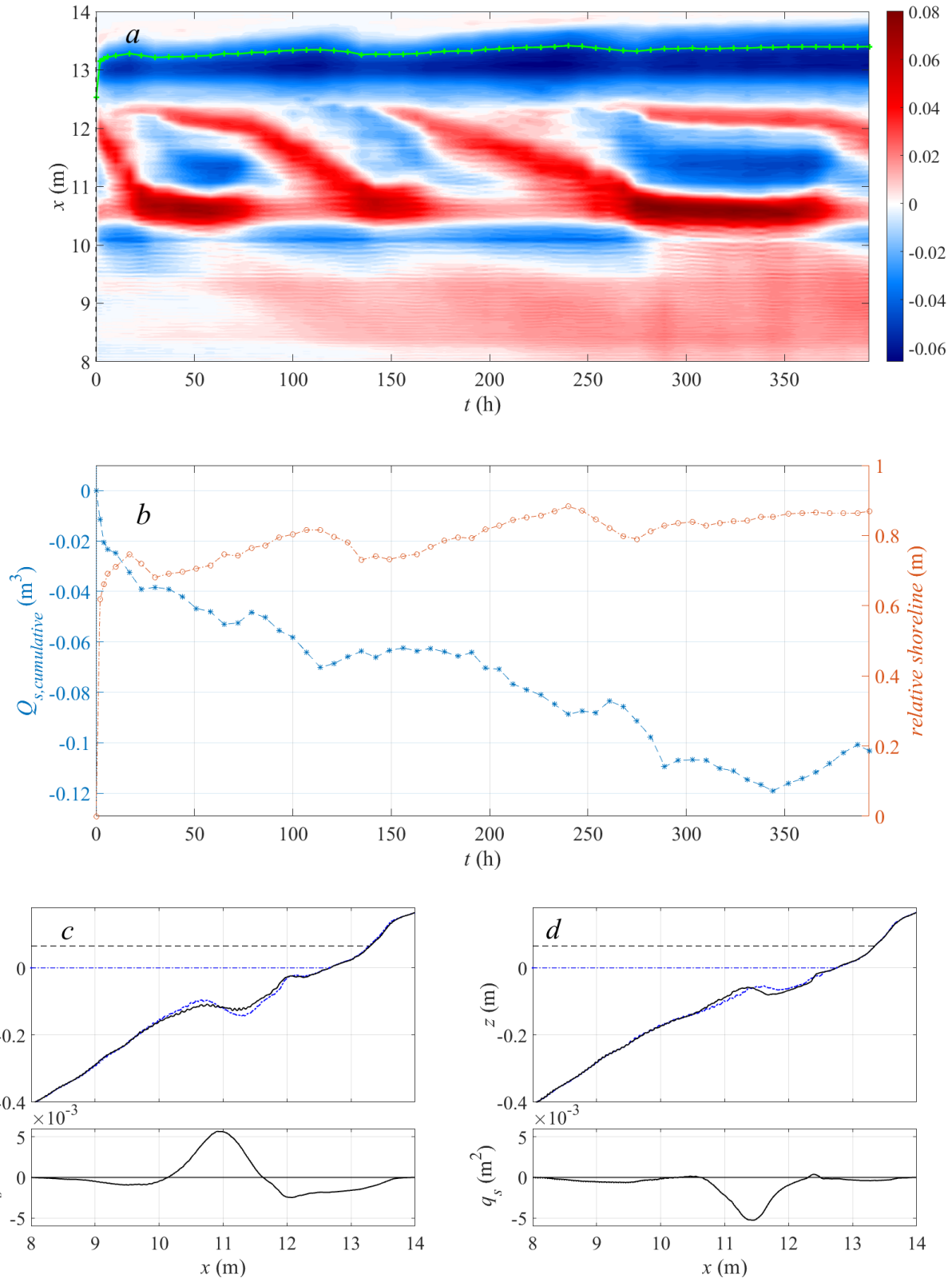

Figure 8: a) Contour plot of profile change versus time for Experiment E-1C. Colour bar in metres. The shoreline is indicated in green with + markers; b) Evolution of cumulative bulk transport, Q_s, and shoreline position versus time. Lower panels: Profile change and sediment transport ($q_s(x)$) between two subsequent profiles during: c) the first bar decay sequence between t = 72 h (blue dashed line) and t = 79 h (black solid line); and d) offshore bar propagation between t = 107 h (blue dashed line) and t = 114 h (black solid line).

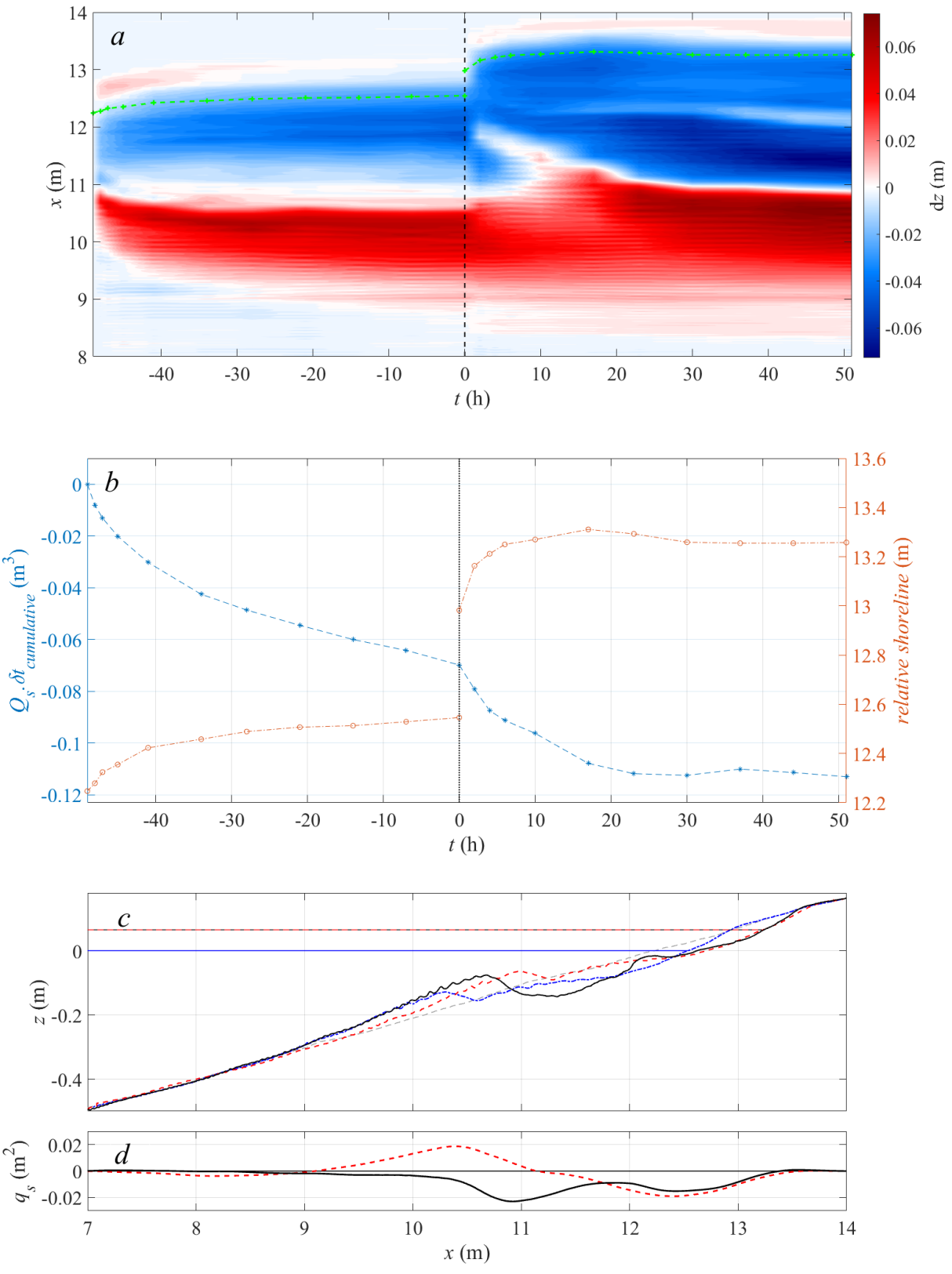

Figure 9: a) Contour plot of profile change versus time for Experiment E-1. Colour bar in metres. The shoreline is dashed green with + markers; b) Evolution of cumulative bulk transport, Q_s, and shoreline position versus time; c) Profile change between the initial planar profile (grey dashed line), final profiles at the initial (blue dashed line) and raised (black solid line) water level, as well as the translated initial water level profile using the PTM (red dashed line); d) Net sediment transport, q_s (x), corresponding to the measured and translated profiles.

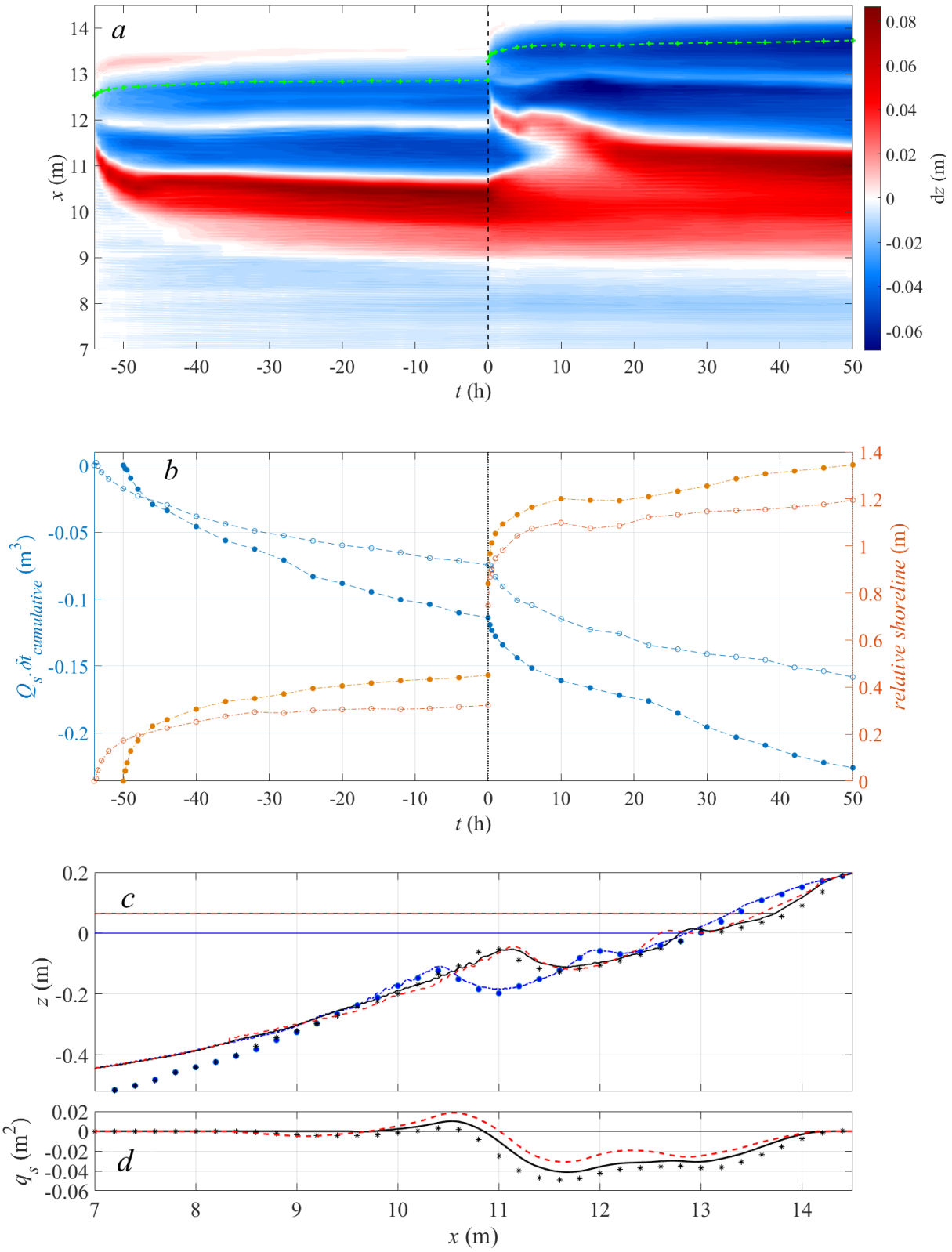

Figure 10: a) Contour plot of profile change versus time for Experiment E-3. Colour bar in metres. The shoreline is dashed green with + markers; b) Cumulative Q_s (blue) and relative shoreline location (orange) before (t<0) and after water level rise for Experiments E-2 (filled circles) and E-3 (open circles); c) Observed and translated profiles for experiment E-3 showing final profiles at initial (blue dash-dot line) and raised (black solid line) water levels and PTM results (red dashed line); d) Net sediment transport, q_s (x), corresponding to the measured and translated profiles. The final profiles before (blue dots) and after (black stars) water level rise and the net-transport distribution are also shown for Experiment E-2.

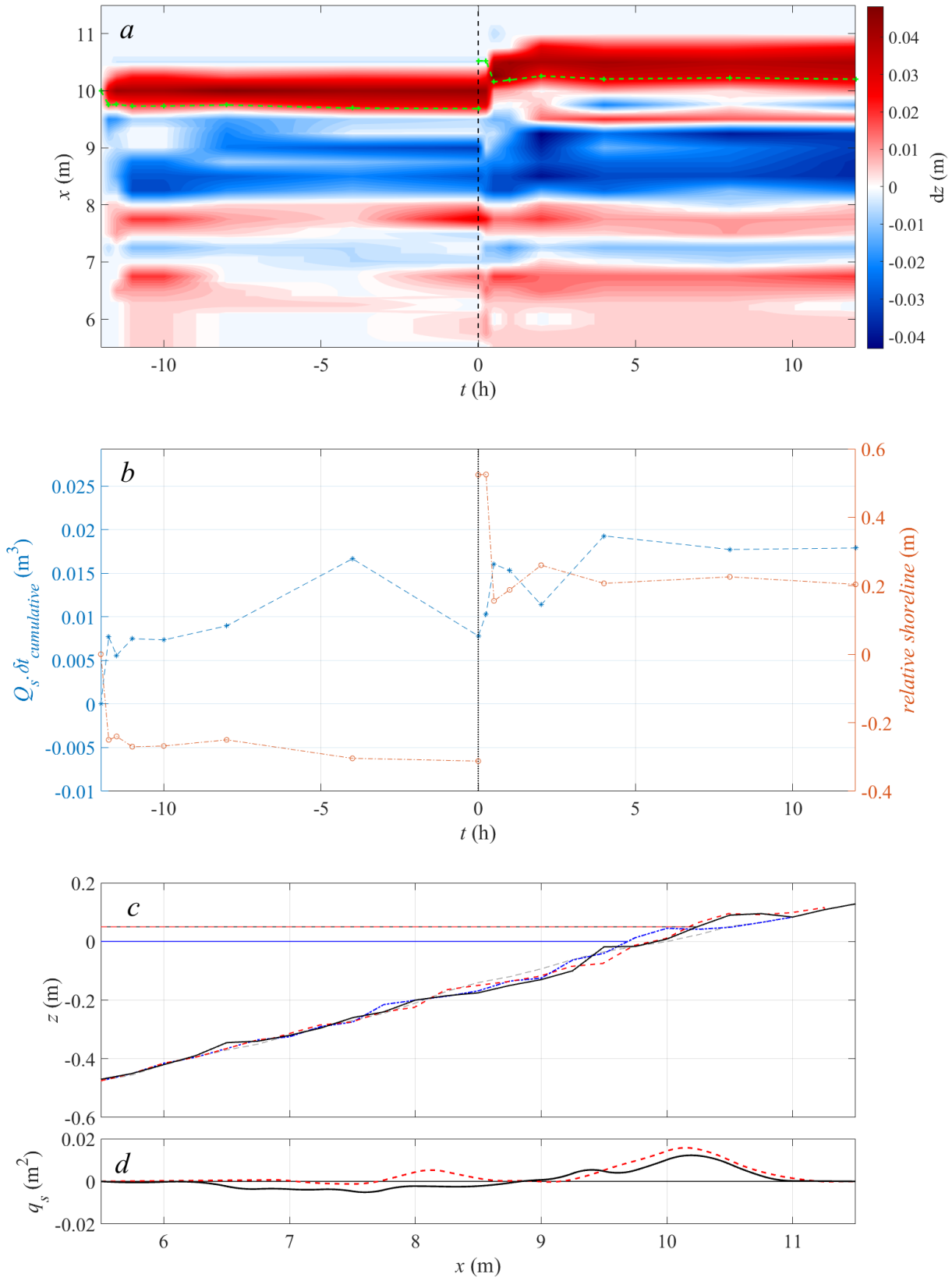

Figure 11: a) Contour plot of profile change versus time for Experiment A-1. Colour bar in metres. The shoreline is green with + markers; b) Evolution of cumulative bulk transport, Q_s, and shoreline position versus time; c) Profile change between the final profiles at the initial (blue dashed line) and raised (black solid line) water level as well as the translated initial water level profile using the PTM (red dashed line); d) Net sediment transport, q_s (x), corresponding to the measured and translated profiles.

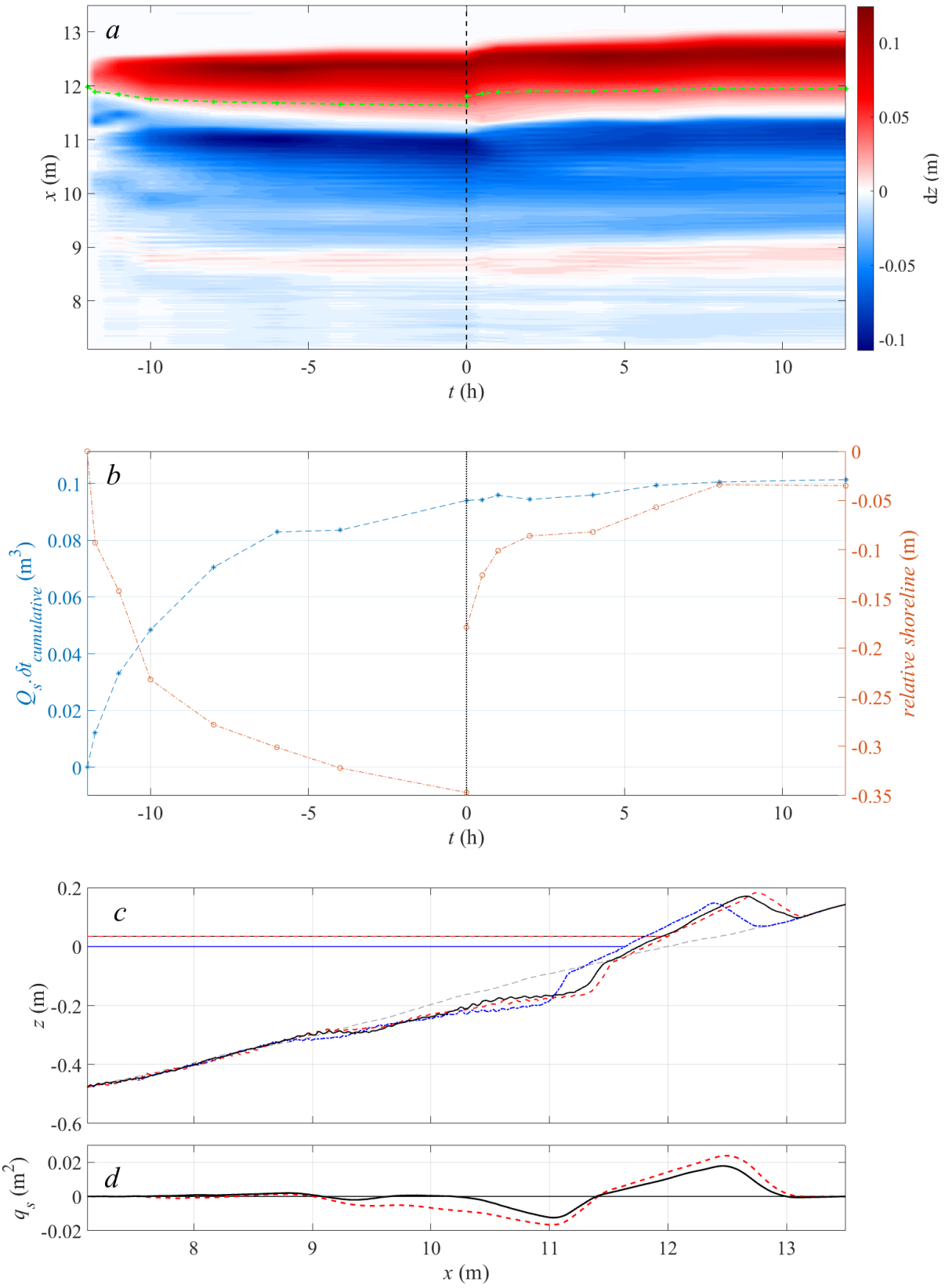

Figure 12: a) Contour plot of profile change versus time for Experiment A-2. Colour bar in metres. The shoreline is green with + markers; b) Evolution of cumulative bulk transport, Q_s, and shoreline position versus time; c) Profile change between the final profiles at the initial (blue dashed line) and raised (black solid line) water levels as well as the translated initial water level profile using the PTM (red dashed line); d) Net sediment transport, q_s (x), corresponding to the measured and translated profiles.

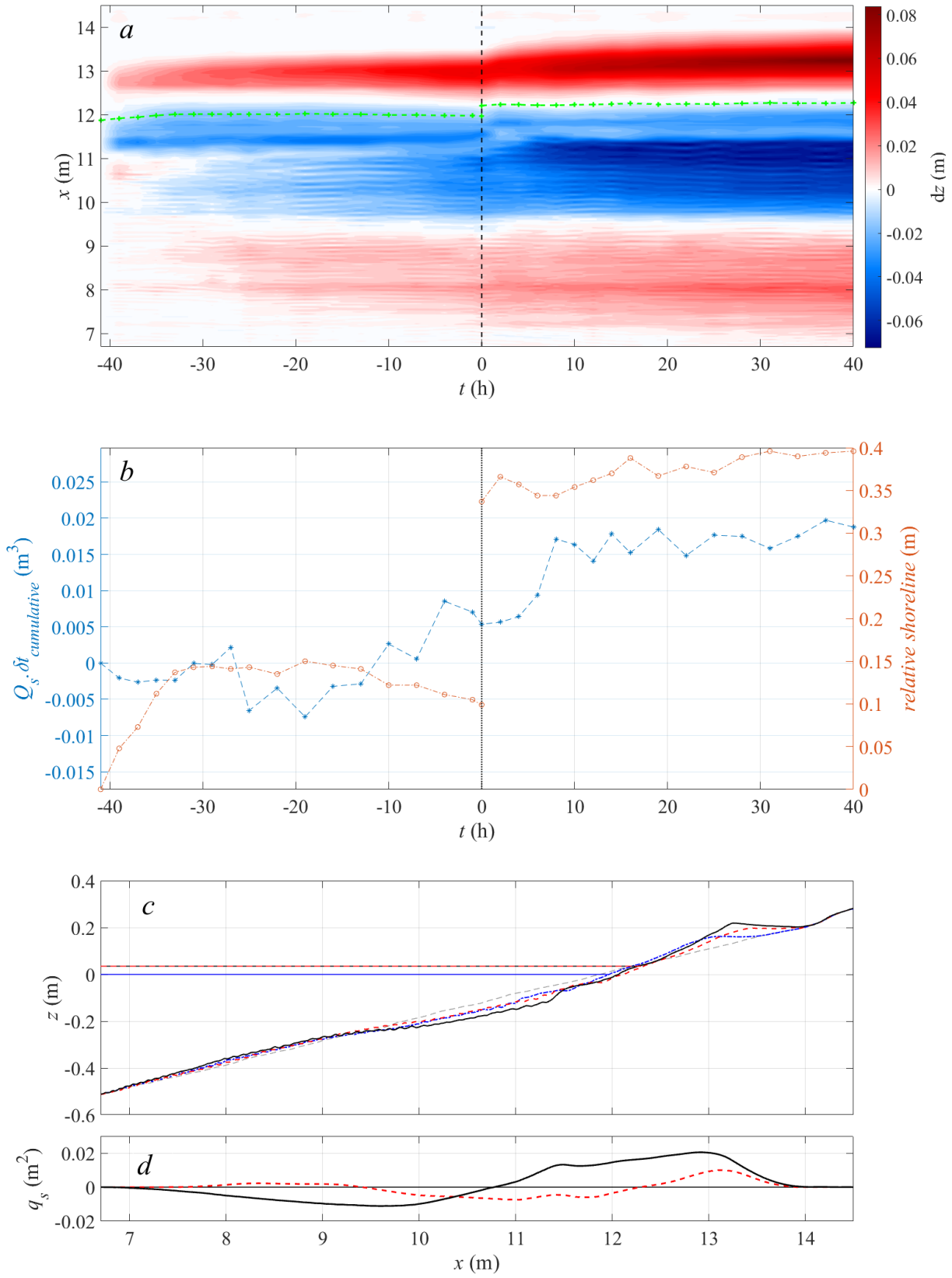

Figure 13: a) Contour plot of profile change versus time for Experiment A-3. Colour bar in metres. The shoreline is green with + markers; b) Evolution of cumulative bulk transport, Q_s, and shoreline position versus time; c) Profile change between the final profiles at the initial (blue dashed line) and raised (black solid line) water level as well as the translated initial water level profile using the PTM (red dashed line); d) Net sediment transport, q_s (x), corresponding to the measured and translated profiles.

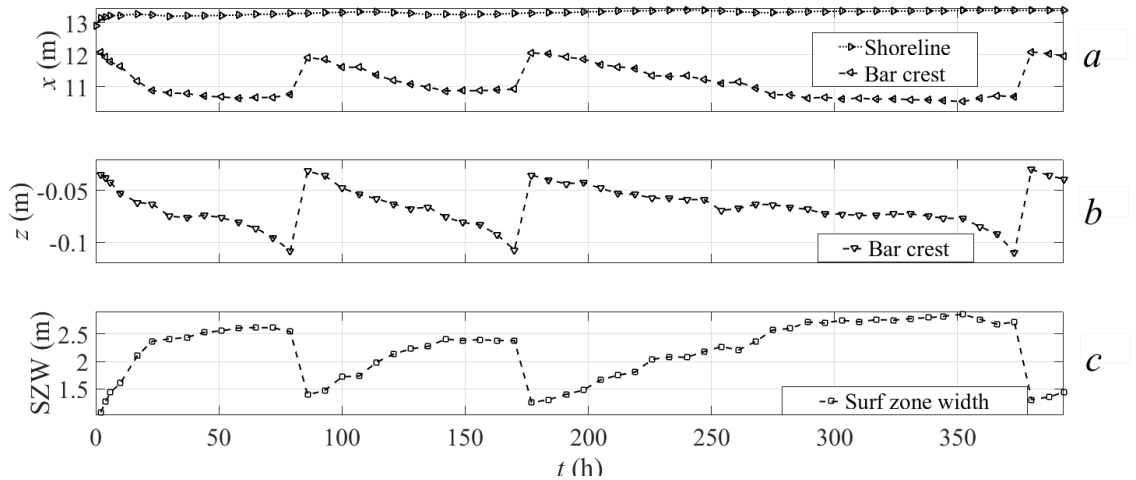

Figure 14: Evolution of profile parameters over time for experiment E-1C. a) Shoreline and bar crest horizontal coordinate location, b) bar crest elevation and c) surf zone width ($x_{shoreline} - x_{bar\ crest}$).

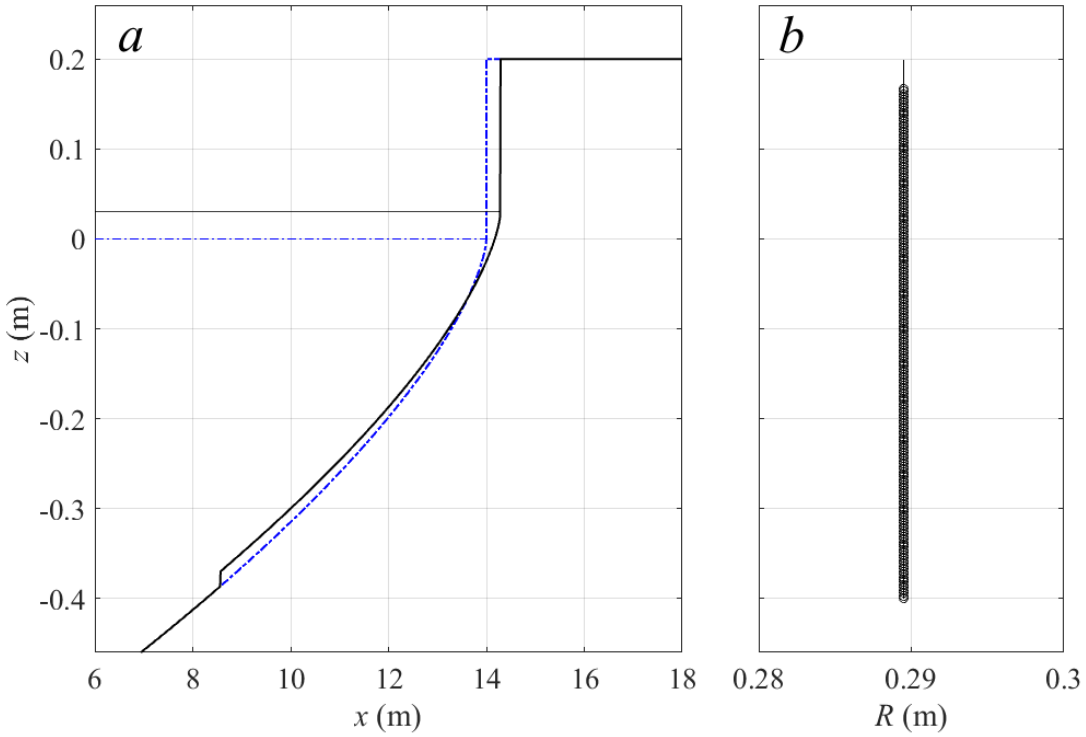

Figure 15: a) Original and translated 2/3-power profile. b) recession at each contour, $R(z)$.

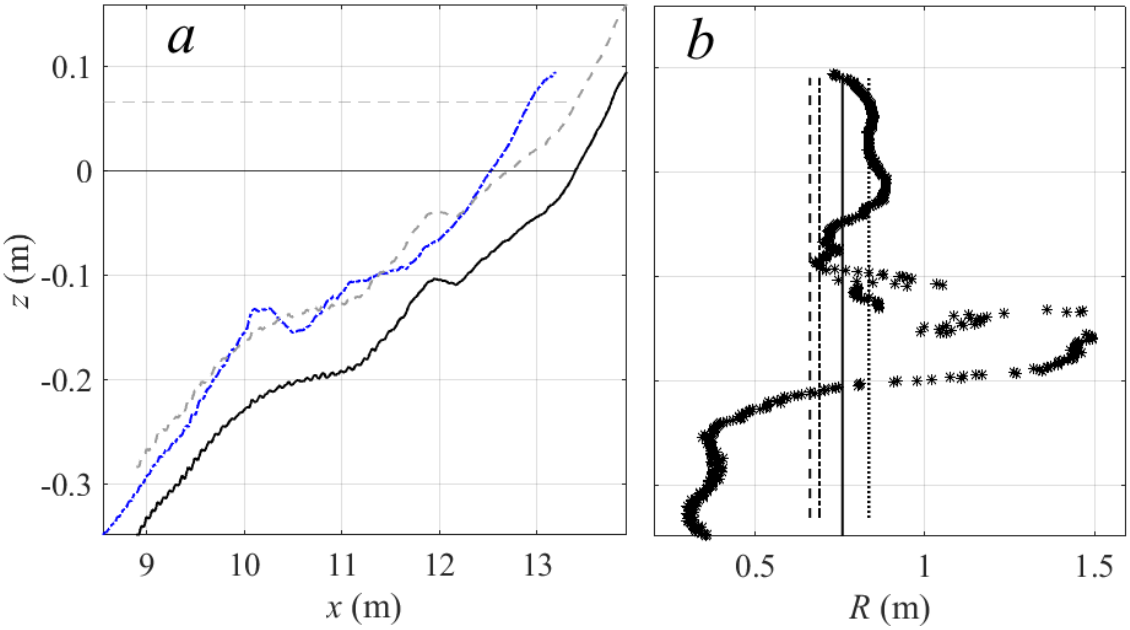

Figure 16: a) Measured E-1C profiles: elevations of the final raised water level profile (dashed grey line) were reduced by -0.065 m (black solid line) to align with the final profile at the initial water level (blue dash-dot line). b) Each discrete contour recession is shown (black stars), along with the mean recession of the profile (solid line), Bruun Rule prediction (dashed line), PTM prediction (dash-dot line) and shoreline recession (dotted line) also indicated.

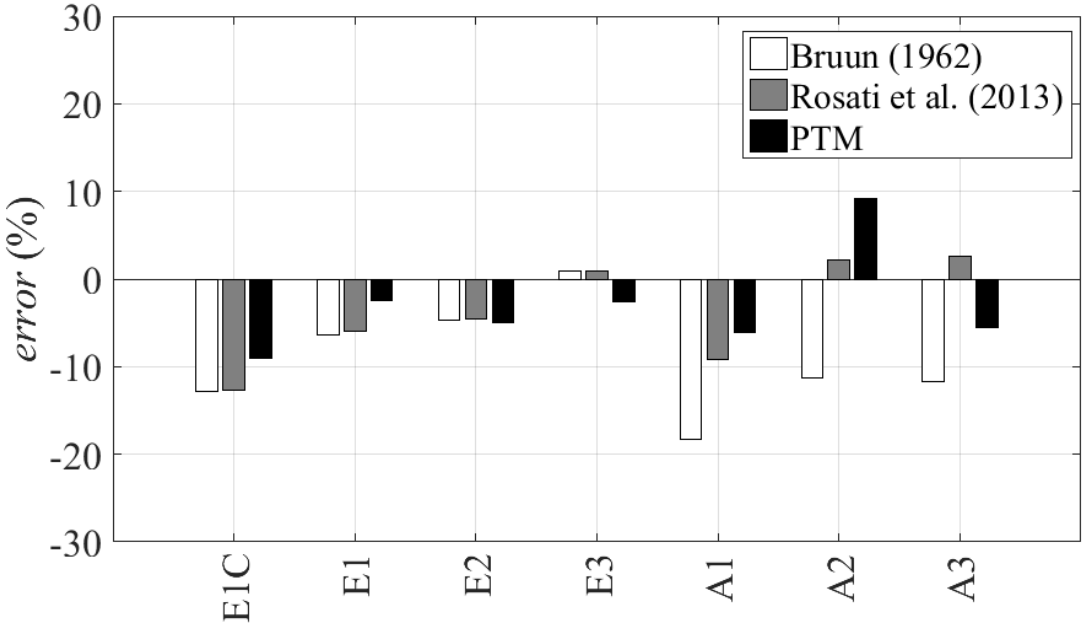

Figure 17: Percentage error of each model with respect to the mean recession of the profile. The vertical axis scale is the same as Figure 9.